Running title: ^{17}O NMR spectroscopy

^{17}O NMR: a "rare and sensitive" probe of molecular interactions and dynamics

Franca Castiglione, Andrea Mele and Guido Raos*

Dipartimento di Chimica, Materiali e Ingegneria Chimica "G. Natta", Politecnico di Milano
Via L. Mancinelli 7, 20131 Milano, Italy

(*) Corresponding author: phone +39-02-2399-3051, email guido.raos@polimi.it

Abstract.
This review summarizes recent developments in the area of liquid-state Nuclear Magnetic Resonance spectroscopy of the ^{17}O nucleus. It is structured in Sections, respectively covering (a) general background information, with special emphasis on spin relaxation phenomena for quadrupolar nuclei and in paramagnetic environments, (b) methods for the calculation of ^{17}O NMR parameters, with illustrative results, (c) applications in chemistry and materials science, (d) application to biomolecules and biological systems, (e) relaxation phenomena, including contrast agents for Magnetic Resonance Imaging (MRI). The ^{17}O nucleus emerges as a very sensitive probe of the local environment ─ including both bonding and non-bonding interactions ─ and molecular motions.

Keywords: chemical shift, relaxometry, quantum chemistry, molecular dynamics, electric field gradient, solvation, imaging, contrast agents, quadrupolar nuclei, oxygen-17.

To be published in vol. 85 of the "ANNUAL REPORTS OF NMR SPECTROSCOPY" (2015).

1. Introduction

The natural history of our planet has followed a path, which has been strongly conditioned by the abundance of water and, after the appearance of photosynthetic organisms, molecular oxygen. Oxygen is an essential element for organic and inorganic chemistry, as well as living organisms and both natural and artificial materials. To the first NMR spectroscopists, it must have been a real disappointment that such a central element has only one rare NMR-active isotope, and that its non-spherical symmetry further increases the difficulty of recording and interpreting its spectra. Thus, for a long time ^{17}O has remained in a niche, often neglected in comparison with simpler and more abundant nuclei. Today, thanks to parallel advances in experimental techniques, theoretical concepts and computational methods, the situation has been partly reversed and ^{17}O NMR spectroscopy is rapidly developing into an important tool for studying the structure and dynamics of oxygen-containing compounds, materials, biological macromolecules and living organisms. The aim of this review is to summarize some of the recent achievements in the field, point out some remaining problems and offer a perspective on possible future developments.

A good entry point to the early literature on chemical applications of ^{17}O NMR spectroscopy is provided by the book edited by Boykin.[1] Gerothanassis[2,3] has authored two comprehensive review articles on ^{17}O NMR, with particular emphasis on a wide range of applications of both liquid and solid-state NMR techniques. Since these reviews cover material published up to 2007, we will mostly concentrate on applications which have appeared from 2008 onwards. Those reviews cover also the experimental methods for the acquisition of ^{17}O NMR spectra and the techniques for the synthesis of ^{17}O-enriched compounds. These will not be discussed here, as there have not been fundamental developments on these fronts. *In vivo* Magnetic Resonance Imaging (MRI) studies of the brain by ^{17}O NMR monitoring of the oxygen metabolic rate have been recently described by Wu and Chen. [4] High-pressure ^{17}O NMR studies of ligand exchange reactions in aqueous metallic cations and polyoxoions have been discussed by Balogh and Casey.[5] More than 50% of the ^{17}O NMR literature concerns solid-state applications, including for example metal oxides, minerals, ceramics, organic crystals, as well as biological macromolecules and materials. These are described in other recent reviews, covering the applications in biology[6-9] and to inorganic and hybrid materials.[10,11] Thus, we will mostly focus on applications in the regimen ranging from liquids to semi-solids, and on theoretical models and computational methods which can be used to interpret these experiments.

This review is organized as follows. Section 2 provides some background information on ^{17}O NMR spectroscopy, focussing in particular on the principles of spin relaxation for quadrupolar nuclei and in paramagnetic species. Section 3 concerns advances in computational methods and illustrates their application to ^{17}O NMR through a number of examples. Section 4 is devoted to applications in chemistry and materials science. Section 5 discusses biochemical and biological systems. Section 6 is devoted to studies and applications of relaxation phenomena. Finally, there is a brief Section with our conclusions.

2. Principles of ^{17}O NMR

This Section establishes a general framework for the discussion of ^{17}O NMR experiments in liquids and semi-solids, including some biological fluids, tissues and organisms. To do so, we summarize material which may be found in several NMR textbooks and review papers. Readers familiar the general principles of ^{17}O NMR spectroscopy may skip this Section and go directly to the following ones, which concentrate on recent results in the field.

2.1 Oxygen NMR parameters

Oxygen has only one NMR-active stable isotope, ^{17}O. This nuclide has a natural abundance of only 0.038%, a nuclear spin quantum number I=5/2, a gyromagnetic ratio γ=-3.628×10^{-7} rad s^{-1} T^{-1} and a Larmor frequency $\omega_0/2\pi$=54.22 MHz (at 400 MHz for ^{1}H).[12] These result in a very low NMR receptivity for the ^{17}O nucleus, compared with other commonly used spin-active nuclei (1.11×10^{-5} and 6.50×10^{-2} times lower than those of ^{1}H and ^{13}C, respectively). Moreover, having a spin quantum number I>1/2, the ^{17}O nucleus has a non-zero electric quadrupole moment. It has a non-spherical, oblate nuclear charge distribution, having a negative quadrupole moment Q=-2.558 fm^2.

The isotropic chemical shift range of ^{17}O spans about 1500 ppm, excluding peculiar but important situations such as O_2 bound to Fe(II) in the haeme group of oxygen-binding proteins (the resonances of the two ^{17}O nuclei fall at about 1700 and 2500 ppm, respectively).[2] Neighbouring elements in the second row of the periodic table have similar or smaller chemical shift ranges (about 220 ppm for ^{13}C in organic compounds, extending up to 400 ppm for ^{13}C bound to metals, 900 ppm for ^{15}N, 1300 ppm for ^{19}F). Figure 1 provides a graphical summary of the typical ^{17}O chemical shifts in some important molecules and functional groups.[8]

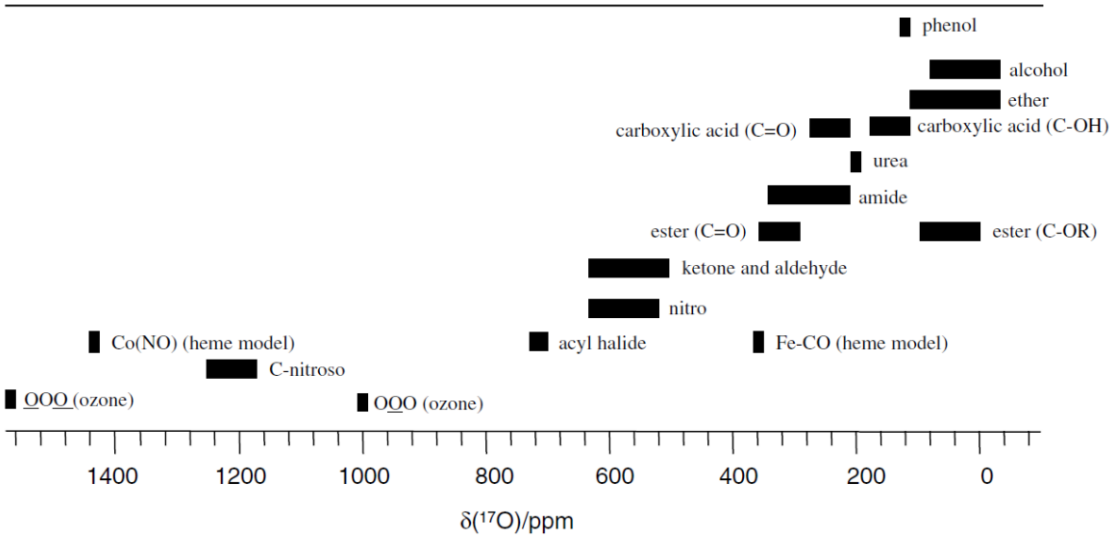

Figure 1: Typical ^{17}O chemical shifts in organic compounds, measured with respect to liquid water (δ=0.0 ppm). Reproduced from ref. 8.

2.2 Nuclear spin interactions

The nuclear Zeeman energy levels for a spin-5/2 nucleus such as ^{17}O are shown in Figure 2. There are six energy levels and five single-quantum transitions. The central transition (CT) between the +1/2 and -1/2 levels is the one usually observed in the NMR experiments of such nuclei. The others are termed first satellite transition (ST_1) and second satellite transition (ST_2). In a strong magnetic field, such as those employed in conventional NMR spectrometers, the other interactions experienced by the nucleus can be seen as perturbations of the Zeeman levels.[13-16]

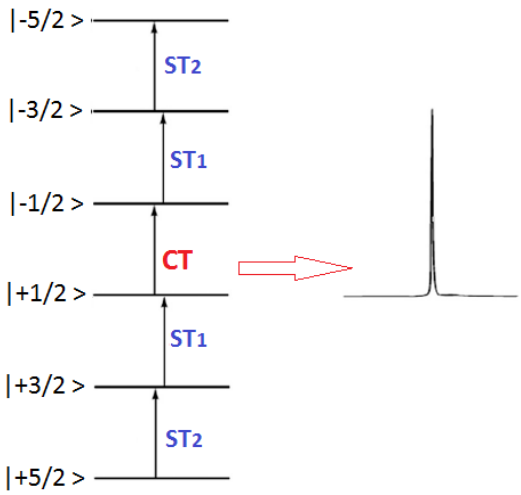

Figure 2: Zeeman energy levels and state labels corresponding to single quantum transitions for *I*=5/2 nuclei. CT = central transition, ST_1 = first satellite transitions, ST_2 = second satellite transitions. Often only the CT is observed.

The general spin Hamiltonian operator which describes an NMR experiment is:[R11-MHL]

$$H = H_Z + H_{CS} + H_J + H_{DD} + H_Q \,. \qquad (1)$$

This holds for closed-shell molecules with no unpaired electrons, when relativistic effects (i.e., spin-orbit coupling) are negligible. The first assumption will be lifted afterwards, when we discuss nuclear spin relaxation in paramagnetic systems. The first two terms in Eq. (1) describe the Zeeman (*Z*) and chemical shielding (*CS*) interactions:

$$H_Z + H_{CS} = -\sum_K \gamma_K \hbar \mathbf{B}^T (1 - \boldsymbol{\sigma}_K) \mathbf{I}_K \qquad (2)$$

where **B** is magnetic induction vector (the *T* superscript indicates the transpose of a vector or matrix), $\mathbf{I}_K$, $\boldsymbol{\sigma}_K$ and γ_K are the spin operator, shielding tensor and gyromagnetic ratio for nucleus *K*. For isotropically tumbling molecules – a legitimate assumption given our focus on solution studies – only the isotropic part of the shielding tensors survives and we have the scalar shielding constants $\sigma_K = Tr(\boldsymbol{\sigma}_K)/3$. These shielding constants are not directly measurable and the results are typically reported as chemical shifts (δ_K) with respect to a suitable reference nucleus (*X*):

$$\delta_K = \frac{\sigma_X - \sigma_K}{1-\sigma_X} = \frac{\nu_K - \nu_X}{\nu_X} \tag{3}$$

where the second expression involves the measured NMR absorption frequencies ν. Water is often used as the solvent in ^{17}O NMR studies and, in such cases, its oxygens represent the natural reference for the evaluation of the chemical shifts. In Section 3.1 we will discuss the absolute shielding scale for ^{17}O, which has relied on a combination of spectroscopic measurements and ab initio calculations.

The two following terms in Eq. (1) describe the indirect (electron-mediated, scalar *J*) and direct dipolar (*DD*) spin-spin couplings:

$$H_J + H_{DD} = \sum_{K>L} \gamma_K \gamma_L \hbar^2 \mathbf{I}_K \left(\mathbf{K}_{KL} + \mathbf{D}_{KL}\right) \mathbf{I}_L \,. \tag{4}$$

In an isotropic solution of freely rotating molecule, the direct dipolar coupling vanishes and we are left with the isotropic part of the indirect coupling tensor (K_{KL}=Tr($\mathbf{K}_{KL}$)/3). This depends only on the electron distribution and can be translated as follows into the conventional coupling constant J_{KL}, which depends on the nuclear gyromagnetic ratios:

$$J_{KL} = \frac{h \gamma_K \gamma_L K_{KL}}{(2\pi)^2}. \tag{5}$$

Finally, the last term in Eq. (1) accounts for the quadrupolar interactions.[16,17] A quadrupolar charge distribution feels the electric field gradient (EFG) around it. If $\phi(x, y, z)$ is the electrostatic potential at (x,y,z), the EFG is a second-rank symmetric tensor **V** with components:

$$V_{\alpha\beta} = -\frac{\partial^2 \phi}{\partial\alpha\partial\beta} \quad \text{with } \alpha, \beta = x, y, z. \tag{6}$$

According to the Laplace equation from classical electrostatics, the trace of this tensor is zero: $V_{xx} + V_{yy} + V_{zz} = 0$. For each nucleus, it is possible to pass from the laboratory reference frame (*x*,*y*,*z*) to a principal axes coordinate system (*X*,*Y*,*Z*), such that the EFG tensor at that nucleus is diagonal and is described by three components $|W_{XX}| \le |W_{YY}| \le |W_{ZZ}|$ (**W**= $\mathbf{R}^{\mathrm{T}}\mathbf{V}\mathbf{R}$, where **R** is a rotation matrix). It is customary to define the two parameters $eq=W_{ZZ}$ and $\eta_q = \frac{W_{XX} - W_{YY}}{W_{ZZ}}$, the latter ranging from 0 to 1.

For each quadrupolar nucleus ($I \ge 1$, $Q \ne 0$), there is a term in the Hamiltonian of the form:

$$H_Q = \frac{eQ}{2I(2I-1)\hbar}\mathbf{I}^T \cdot \mathbf{V} \cdot \mathbf{I} \qquad (7)$$

where e is the elementary charge. In solids under typical experimental conditions (strong field limit), this can be simplified as it acts as a perturbation with respect to the Zeeman term, but it is still larger than the remaining ones. The first-order term in the resulting Hamiltonian is proportional to the quadrupolar coupling constant $C_q = \frac{eQeq}{h}$. Figure 3 shows that, much like the chemical shifts, also the quadrupolar coupling constants are fairly transferable among similar groups.

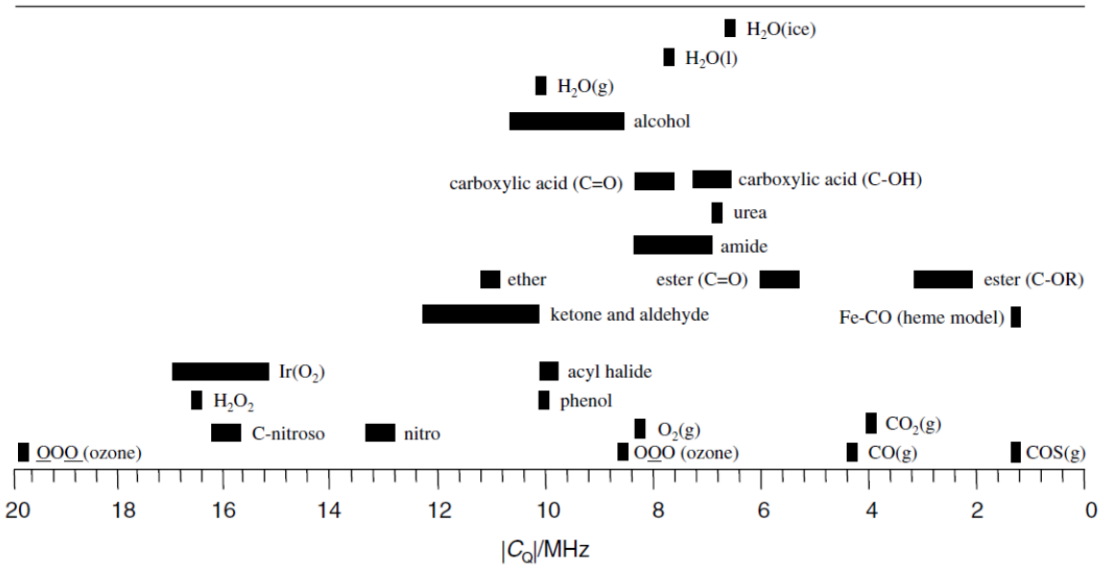

Figure 3: Typical ^{17}O quadrupolar coupling constants in organic compounds. Reproduced from ref. 8.

In isotropic liquids and solutions, the quadrupolar interactions are averaged to zero by rapid molecular tumbling and the ^{17}O spectrum is dominated by the chemical shielding terms. However, the interaction between the nuclear quadrupole moment and the fluctuating EFG at that nucleus has still a major effect on the NMR spectrum, as it provides a fast spin relaxation mechanism, leading to characteristically broad lines. In the following section we introduce some elements of the theory of relaxation of quadrupolar nuclei, in preparation for the discussion of recent experiments on ^{17}O-containing systems.

2.3 Quadrupole relaxation theory

Relaxation is a key phenomenon for magnetic resonance and there is an extensive literature covering its theoretical and experimental aspects.[13-16] The transverse or spin-spin relaxation rate $R_2=1/T_2$ determines the widths of the resonances in the spectrum, the longitudinal or spin-lattice relaxation rate

$R_1=1/T_1$ determines the minimum time delay needed between two acquisitions. Relaxation can provide valuable information on molecular motions and intramolecular distances and is extensively exploited in MRI.

In liquids, the nuclear electric quadrupole interaction provides the dominant relaxation mechanism for spins $I>1/2$. Since the nuclear quadrupole Q is effectively constant in magnitude, the fluctuations in this interaction are determined by the orientation, magnitude and temporal average of the EFG. This is mainly intramolecular in origin, as the EFG produced by a point charge q (e.g., some neighbouring nucleus) decays with distance as q/r^3. This observation arises also from the transferability of the quadrupolar coupling constants among oxygens in similar bonding environments (see again Figure 3). The tumbling or random reorientation of a molecule in solution produces a torque on its quadrupolar nuclei, changing their alignment with respect to the external magnetic field. The quadrupolar coupling constant C_q and the asymmetry parameter η_q introduced in the previous section can be directly determined from the analysis of the NMR spectrum and they are related to the quadrupole product parameter, $P_q = C_q\sqrt{1+\frac{{\eta_q}^2}{3}}$.

The relaxation behaviour of a system strongly depends on its motional regime, giving rise to different features in the NMR spectrum. In the following we describe two possible regimes and their effects on the spectra for a single type of oxygen, assuming that the motion can be characterized by a single correlation time τ_c.[18]

2.3.1 Isotropic motion with motional narrowing ($\omega_0\tau_c << 1$)

In a quadrupolar system undergoing rapid motion, such as in a small molecule in solution, the longitudinal (R_1) and transverse (R_2) relaxation rates for the single quantum transitions between the ($2I$ + 1) Zeeman levels are identical (see again Figure 2). The magnetization decays monoexponentially, giving a single Lorentzian peak with a width $\Delta\upsilon_{1/2}$ given by:

$$R_1 = R_2 = \Delta\upsilon_{1/2} = \frac{12\pi^2}{125}{P_q}^2\tau_c . \qquad (8)$$

The relaxation rate can then be estimated by measuring the peak width $\Delta\upsilon_{1/2}$ in the NMR spectrum. Narrow lines can be expected for small molecules in non-viscous fluids or for small C_q values. The P_q and τ_c parameters may be obtained in turn by combining independent estimates of the EFG or of the characteristic time for molecular reorientation (from NMR experiments on other nuclei, quantum chemical calculations or molecular dynamics simulations, for example).

2.3.2 Isotropic motion in the intermediate to slow motion regimes ($\omega_0\tau_c \approx 1,\ \omega_0\tau_c > 1$)

In the intermediate and slow motion regimes, which apply to many biological macromolecules, the satellite and central transitions have different longitudinal and transverse relaxation rates. Therefore the time evolution of the total transverse magnetization is described by a weighted sum of (I+1/2) complex exponentials, respectively for the CT, ST1 and ST2 transitions:

$$M_{(x,y)}(t) = \sum_{i=1}^{3} A_i^{(2)} \exp\left[-\left(i\Omega_i + R_{2,i}\right)t\right] \tag{9}$$

Similarly, the recovery of the longitudinal magnetization has three exponential components:

$$M_{(z)}(t) - M_{(z)}(t=\infty) = \sum_{i=1}^{3} A_i^{(1)} \exp\left(-R_{1,i}t\right) \tag{10}$$

where $A_i^{(2)}$ and $A_i^{(1)}$ are the amplitudes of the ith component, $\sum_{i=1}^{3} A_i^{(2)} = \sum_{i=1}^{3} A_i^{(1)} = 1$ and Ω_i is the dynamic (angular) frequency shift. Each of these exponential functions corresponds to a resonance in the spectrum, but some of these (always ST2, usually also ST1) are too broad to be observed.

A general analytical expression for the amplitudes and relaxation rates has not been derived. However these quantities have been obtained by numerical calculations[19-21] based on the Redfield relaxation theory.[22] The theoretical NMR spectra calculated for a spin 5/2 nucleus over a broad range of molecular motions ($0.1 \le \omega_0\tau_c \le 20$) are shown in Figure 4.a).[21] As can be seen, when $\omega_0\tau_c \approx 1$ the three components give comparable contributions to the spectrum, the absorption peak is not Lorentzian and as a result it makes little sense to obtain an overall relaxation rate from the measurement of the peak width. Instead, for small $\omega_0\tau_c$ values (extreme narrowing condition) as well as for large $\omega_0\tau_c$ values (slow motion), the spectrum shows a single Lorentzian line. The high resolution achievable in the slow motion regime is surprising at first. It depends on the fact that the two satellite transitions are too broad to be detectable, while the CT transition occurs at a sufficiently small rate to lead to a sharp peak again. Westlund and Wennerstroem[23] derived the analytical expression for the transverse relaxation rate of the CT for spin 5/2 or spin 7/2 nuclei in the isotropic slow motion limit. The line width at half height is:

$$\Delta\upsilon_{1/2} = 7.2 * 10^{-3}\left(\frac{P_q}{\upsilon_0}\right)^2 \frac{1}{\tau_c} \tag{11}$$

Comparison with the expression in the motional narrowing regime of Eq. (8) shows that, even though both peaks are Lorentzian, the width now depends on the nuclear resonance frequency υ_0 (the lines become narrower on increasing the static magnetic field) and is inversely proportional to τ_c.

Another important feature, in this window of molecular motion, is that the NMR signal is also modified by a shift change, the second order dynamic frequency shift. Its analytical expression has been given by Werbelow et al.:[24,25]

$$\Delta\delta = -6*10^{3}\left(\frac{P_q}{\upsilon_0}\right)^2 \qquad (12)$$

This is an up-field shift whose magnitude decreases on increasing the external field B_0. Since this also depends on P_q, its measurement can be combined with that $\Delta\upsilon_{1/2}$ to obtain both this parameter and dynamic information (τ_c).

A recent paper by Zhu et al.[26] has provided an experimental demonstration of these predictions for the ^{17}O quadrupolar relaxation properties over the entire range of molecular motion, from the extreme narrowing to the slow motion limit. The two ^{17}O resonances of neat liquid glycerol ($OHCH_2CH(OH)CH_2OH$) have been monitored at very high fields (B_0=21.14 T, corresponding to a Larmor frequency $\omega_0/2\pi$=122 MHz) over a range of temperatures, from 240 to 340 K (Figure 4.b)). The lowest temperature correspond to a strongly supercooled state. Temperature has a strong effect on molecular motion and both the liquid viscosity and the correlation time τ_c change by four orders of magnitude in this range. As τ_c increases on lowering the temperature, the NMR signal initially become very broad. However at very low temperatures two sharp lines reappear, providing the experimental verification of the theoretical prediction of the relaxation properties. Notice also the dynamic frequency shift, so that the peaks move from negative to positive δ's on decreasing the temperature.

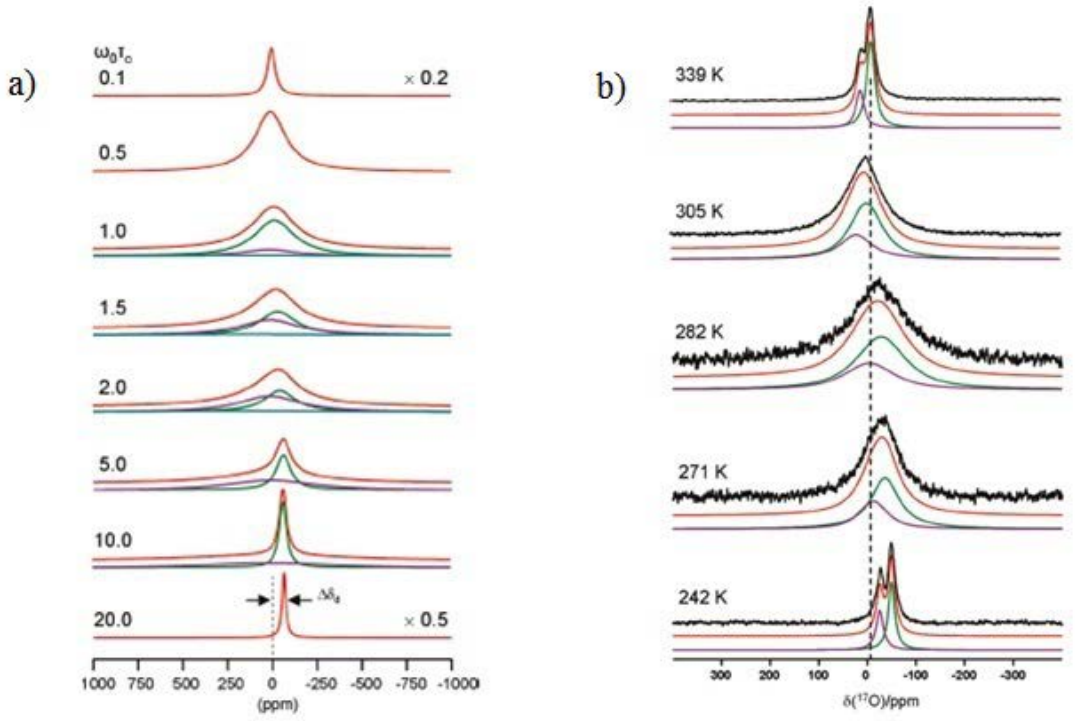

Figure 4: a) Theoretical ^{17}O line shapes as a function of $\omega_0\tau_c$. All spectra were calculated assuming P_q = 8.5 MHz, δ_{iso} = 0 ppm, and ν_0 =81.36 MHz (14.09 T). The total line shapes are shown in red, and individual components are shown in green (CT), blue and purple. Reproduced from ref. 21. **b)** Experimental (upper traces) and simulated (lower traces) ^{17}O NMR spectra of glycerol at 21.14 T and different temperatures. Reproduced from ref. 26.

The results of Eqs. (11) and (12) have been derived on the basis of Redfield's theory,[22] and because of the assumptions in that theory they are valid as long as $\omega_0\tau_c$ remains smaller than $\left(\frac{\omega_0}{2\pi C_q}\right)^2$.[21] For very slow motions that are beyond this range, higher order effects become important.[27] In the intermediate-slow motion limit, which applies to many biological macromolecules, additional interactions such as the shielding anisotropy (SA) may contribute to the transverse relaxation mechanism, and thus increase the experimental line width. Studies by Lerner and Torchia[28] have shown the importance of the SA contribution to the multiexponential quadrupolar relaxation processes and a detailed theoretical development has been reported by Spiess.[29]

2.4 Relaxation in paramagnetic systems

As we shall see, ^{17}O NMR can be employed to study the interaction of water molecules or oxygen-containing ligands with transition metal ions. Many of these studies are motivated by the search of improved contrast agents for MRI (see Section 6 for specific examples). In these paramagnetic systems, the dominant relaxation mechanisms may be attributed to the interaction between the fluctuating magnetic field of the unpaired electron(s) and the resonating nuclei, and to the time dependence of the parameters associated with the interaction.[30-33] These increase both the longitudinal (R_1) and transverse (R_2) nuclear spin relaxation rates, an effect that is commonly called Paramagnetic Relaxation Enhancement (PRE).

The diamagnetic and paramagnetic contributions to the relaxation rates of such solutions are additive and given by: $\left(\frac{1}{T_i}\right)_{obs} = \left(\frac{1}{T_i}\right)_d + \left(\frac{1}{T_i}\right)_p$ (i = 1 or 2), where $\left(\frac{1}{T_i}\right)_{obs}$ is the observed solvent relaxation rate in the presence of a paramagnetic species, $\left(\frac{1}{T_i}\right)_d$ is the solvent relaxation rate in the absence of a paramagnetic species, and $\left(\frac{1}{T_i}\right)_p$ represents the additional paramagnetic contribution. In a dilute solution, the latter is proportional to the concentration of the paramagnetic species [M]:

$$\left(\frac{1}{T_i}\right)_{obs} = \left(\frac{1}{T_i}\right)_d + r_i[M] \quad (i = 1, 2). \tag{13}$$

The slopes r_i are the relaxivities, with units $mM^{-1}s^{-1}$. They are usually measured over a wide range of Larmor frequencies and at several temperatures. Curves showing the r_i's are called nuclear magnetic relaxation dispersion (NMRD)[34] curves or relaxometry profiles.

The enhanced relaxation provided by a paramagnetic center is linked to a combination of phenomena, including random diffusion of the solvent and the metal's coordination complex and specific chemical interactions that occur when they approach each other. The total relaxivity r_i consists of three contributions: 1) inner-sphere (IS), from the solvent molecules that are directly coordinated to the metal ion, 2) second sphere (SS), from the molecules interacting with the ligand structure, for example through hydrogen bonding, 3) outer-sphere (OS), from the molecules diffusing in close proximity of the complex. The IS and SS contributions are not always distinguishable, while the third one is usually small and often neglected. The IS relaxation contribution depends on the exchange of water molecules between the primary coordination sphere of the ion and the bulk solvent, leading to the equation:

$$\left(\frac{1}{T_1}\right)_{IS} = \frac{\chi_M b}{T_{1M} + \tau_M} \ . \tag{14}$$

Here χ_M is the mole fraction of metal ions and b is the number of bound water molecules per metal ion (so that their product is the fraction of bound molecules), T_{1M} is the relaxation time of the bound water, and τ_M is the residence lifetime of the bound water. This equation is valid independently of the regime of exchange between the complex and the free ligand and independently of the difference in resonance frequency between the free and bound ligand $\Delta\omega_M$. For the transverse relaxation, a similar equation is valid only when $\Delta\omega_M << \frac{1}{T_{2M}}$, otherwise a more complex relation is used. The relaxation rates $\frac{1}{T_{1M}}$ and $\frac{1}{T_{2M}}$ are given in turn by the Solomon-Bloembergen-Morgan (SBM) theory.[35,36] They are composed of contributions from the contact ($\frac{1}{T_{i,C}}$, also known as hyperfine or scalar), the dipolar ($\frac{1}{T_{i,D}}$) and the Curie ($\frac{1}{T_{i,\chi}}$) mechanisms. These are individually discussed below, alongside some notable experimental results. Further results on the water exchange mechanisms in transition metal complexes are discussed in Section 6.2.

The contact contribution, due to the through-bond interactions, is given by:

$$\frac{1}{T_{1,C}} = \frac{S(S+1)}{3}\left(\frac{A}{\hbar}\right)^2\left(\frac{2\tau_e}{1+\omega_S^2\tau_e^2}\right) \tag{15a}$$

$$\frac{1}{T_{2,C}} = \frac{S(S+1)}{3}\left(\frac{A}{\hbar}\right)^2\left(\tau_e + \frac{\tau_e}{1+\omega_S^2\tau_e^2}\right) \qquad (15b)$$

$$\frac{1}{\tau_e} = \frac{1}{\tau_M} + \frac{1}{T_{ie}}, \qquad (i=1,2) \qquad (15c)$$

where S is the total spin quantum number of the paramagnetic centre, T_{1e} and T_{2e} are the electron relaxation times and ω_S is the Larmor angular frequency for the electron. The contact interaction is independent of molecular tumbling and the magnitude of $\frac{1}{T_{2,C}}$ is usually governed by T_{2e} and the hyperfine coupling constant ($A/\hbar$), whose values depend on the electron delocalization from the paramagnetic centre to the nucleus under study.

^{17}O relaxation measurements have recently been applied to study the hydration state of the Mn(II) ion in coordination complexes and metalloproteins.[37] This is a high spin d^5 cation (S=5/2), which may easily adopt different coordination geometries. The paramagnetic contribution to the transverse relaxation rate has been measured from the line width of the $H_2{}^{17}O$ signal in aqueous Mn(II) solutions. According to Eq. (14), in the fast exchange regime, the number of bound water molecules b can be directly determined from the experimental data, considering that the contact term represents the dominant relaxation mechanism. For the Mn(II) ion, the electronic relaxation time T_{ie} increases with the square of the applied magnetic field,[38] thus at high magnetic fields the $\frac{1}{T_{ie}}$ term can be neglected and the correlation time for the scalar relaxation will be the water residence time τ_M. Under the condition of maximum paramagnetic ^{17}O relaxation rate, $T_{2M} = \tau_M$ and the average number of bound water molecules is simply proportional to the transverse oxygen relaxivity:

$$b \cong \frac{r_{2\max}^{O}}{510}$$

where the proportionality factor is obtained using $\frac{A_O}{\hbar} = 3.3\times10^7$ rad/s for the hyperfine coupling constant for Mn(II)-$^{17}OH_2$ (this value does not depend much on the presence of other ligands). This methodology has given accurate estimates of b for several aqueous Mn(II) complexes and metalloproteins, with uncertainties of ±0.2 water molecules. Moreover, the contact relaxation mechanism is related to the water exchange rate constant, whose temperature dependence follows the Eyring equation:

$$\frac{1}{\tau_M} = k_{ex} = \frac{k_B T}{h}\exp\left\{\left(\frac{\Delta S^{\ddagger}}{R}\right) - \left(\frac{\Delta H^{\ddagger}}{RT}\right)\right\} \qquad (16)$$

thus allowing the determination of the activation enthalpy $\Delta H^{\ddagger}$ and entropy $\Delta S^{\ddagger}$ for water exchange.

The dipolar contribution results from the through-space electron-nucleus interactions and is described by the equations, assuming isotropic reorientation of the complex:

$$\frac{1}{T_{1,D}} = \frac{2}{15}\left(\frac{\mu_0}{4\pi}\right)^2 \frac{\gamma_I^2 \mu_{eff}^2 \ \beta^2}{r^6}\left(\frac{3\tau_c}{1+\omega_I^2\tau_c^2} + \frac{7\tau_c}{1+\omega_S^2\tau_c^2}\right) \tag{17a}$$

$$\frac{1}{T_{2,D}} = \frac{1}{15}\left(\frac{\mu_0}{4\pi}\right)^2 \frac{\gamma_I^2 \mu_{eff}^2 \ \beta^2}{r^6}\left(4\tau_c + \frac{3\tau_c}{1+\omega_I^2\tau_c^2} + \frac{13\tau_c}{1+\omega_S^2\tau_c^2}\right) \tag{17b}$$

where μ_0 is the vacuum permeability, γ_I is the magnetogyric ratio, μ_{eff} is the effective magnetic moment of the paramagnetic ion, β is the Bohr magneton, r is the distance between the nucleus under study and the paramagnetic ion, ω_I and ω_S are the Larmor angular frequencies of the nucleus and the electron and τ_c is the correlation time. The latter is given by:

$$\frac{1}{\tau_c} = \frac{1}{\tau_M} + \frac{1}{T_{1e}} + \frac{1}{\tau_R} \tag{18}$$

where now appears τ_R, the rotational tumbling time of the complex in water. Typical values are τ_R=10^{-10}-10^{-11}s for low molecular weight complexes in water, and τ_M>10^{-9} s. When ω_I and ωs are much smaller than $\frac{1}{\tau_c}$, in the fast motion limit, the Solomon equations reduce to:

$$\frac{1}{T_{1,D}} = \frac{2}{5}\left(\frac{\mu_0}{4\pi}\right)^2 \frac{\gamma_I^2 \mu_{eff}^2 \ \beta^2}{r^6}\tau_c\,, \tag{19a}$$

$$\frac{1}{T_{2,D}} = \frac{7}{15}\left(\frac{\mu_0}{4\pi}\right)^2 \frac{\gamma_I^2 \mu_{eff}^2 \ \beta^2}{r^6}\tau_c\,. \tag{19b}$$

In this approximation, $\tau_c \approx \tau_R$ and the rotational motion of the complex can be determined directly from the experimental data.

The Curie mechanism accounts for the interaction between the nuclear spin and the time-averaged electron spin moment. This process is modulated by the rotational motion of the complex and plays a role only when the correlation time τ_R is four orders of magnitude larger than T_{1e}. The Curie spin terms can be expressed as:

$$\frac{1}{T_{1,\chi}} = \frac{6}{5}\left(\frac{\mu_0}{4\pi}\right)^2 \frac{\gamma_I^2 H_0^2 \mu_{eff}^4 \ \beta^4}{(3kT)^2 r^6}\left(\frac{\tau_R}{1+\omega_I^2\tau_R^2}\right) \tag{20a}$$

$$\frac{1}{T_{2,\chi}} = \frac{1}{5}\left(\frac{\mu_0}{4\pi}\right)^2 \frac{\gamma_I^2 H_0^2 \mu_{eff}^4 \ \beta^4}{(3kT)^2 r^6}\left(4\tau_R + \frac{3\tau_R}{1+\omega_I^2\tau_R^2}\right) \qquad (20b)$$

where H_0 is the applied magnetic field. The contribution of this mechanism to the total longitudinal relaxation is significant only for slowly tumbling molecules at high magnetic fields and it is usually difficult to measure, due to the predominance of the other two. Recently, Mareš et al.[39] have bypassed the experimental difficulties by computing the Curie contribution to the PRE for Ni(II) in aqueous solution, which is interesting as a model system for several paramagnetic NMR relaxation studies. They did this by combining molecular dynamics simulations, quantum chemical calculations on snapshots of the Ni(II) ion with its first solvation shell and the Redfield relaxation theory. The Curie term has been estimated to contribute to the total ^{17}O relaxation rates by 33 s^{-1} for R_1 and 38 s^{-1} for R_2, in an 11.7 T magnetic field. These are indeed very small numbers, in comparison to the contact and dipolar contributions.

The outer-sphere (OS) relaxation contribution is more complex and depends on the diffusion coefficient of the both the solvent and the complex, for this reason it is often neglected in relaxation studies. However, this mechanism becomes important in the case of contrast agents for MRI. These reagents typically have only one water molecule in the inner coordination sphere, so that the contribution of the outer sphere relaxation can be relatively large. Several studies have been performed by Aime et al.[40] in order to obtain new contrast agents with higher OS relaxation.

3. Calculation of ^{17}O NMR parameters

The evaluation of the shielding constants by quantum-chemical methods is a now mature subject, to the point that it has become accessible also to non-specialists. It is increasingly common for experimentalists to use some kind of ab initio calculation to validate or rationalize their measurements, without resorting to chemical shift compilations and databases, especially for relatively exotic nuclei such as ^{17}O which have not been studied as extensively as ^{1}H or ^{13}C. Because of this, and of the obvious interest to the theoretical community, it seems appropriate to discuss here some recent successful applications of these computational methods. After the chemical shifts, we go on to discuss the calculations of spin-spin coupling constant involving ^{17}O and of the EFG's, which are relevant for relaxation phenomena and the NMR line widths.

3.1 Chemical shifts

A thorough, still useful review of the theoretical principles underlying ab initio calculations the nuclear shielding and indirect or scalar-*J* nuclear spin couplings was written some years ago by Helgaker, Jaszunski and Ruud.[41] Since then, Oldfield[42] has reviewed the application of these methods to problems in structural biology, Casablanca and de Dios[43] have authored a brief commentary on recent methodological progress, while Benzi at al.[44] have provided an introduction to the quantitative inclusion

of solvent effects. Even more recent reviews are those of Vaara,[45] Facelli[46] and Lodewyk, Siebert and Tantillo.[47] The first one emphasizes advances in non-standard applications (relativistic effects, open-shell molecules, non-linear response at very high magnetic fields, etc.), the second one discusses the problems which arise in the calculation of the full shielding tensors (appropriate for solids), and the last one provides a tutorial introduction to these calculations, focussing in particular on ^{1}H and ^{13}C chemical shifts. All of them provide some general guidelines (expected accuracies for different computational levels, possible sources of error, etc.) which should be applicable also to ^{17}O chemical shifts. The computational methods necessary for the treatment of periodic systems with a plane wave basis set are quite distinct from the more traditional ones with localized basis sets and they have also been reviewed recently, together with many applications.[48] Further developments within the broader field of computational NMR spectroscopy may be found in an edited book.[49]

In his seminal work, Ramsey analysed nuclear shielding in molecules from the point of view of quantum mechanical perturbation theory.[50] He identified a first- and second-order contribution, which correspond to a positive diamagnetic term and a negative paramagnetic one:

$$\boldsymbol{\sigma}_K = \boldsymbol{\sigma}_K^{dia} + \boldsymbol{\sigma}_K^{para} \tag{21}$$

The explicit expressions show that first one can be easily evaluated from the ground state electronic wave function, but the second one would require knowledge of all the excited singlet states, which is extremely difficult to obtain for all but the simplest model systems. Modern quantum-chemical methods for the evaluation of the shielding constants are rooted in the identification of these quantities with the second derivatives of the energy of a molecular system with respect to the magnetic induction **B** and the nuclear moments $\mathbf{M}_K=\hbar\gamma_K\mathbf{I}_K$:[41]

$$\boldsymbol{\sigma}_K = \mathbf{1} + \left.\frac{\partial^2 E}{\partial \mathbf{B}\partial \mathbf{M}_K}\right|_{\mathbf{B}=0,\mathbf{M}_{J\neq K}=0} \tag{22}$$

where **1** is the 3×3 unit matrix. Analytical formulae for these derivatives have been obtained and programmed, for both variational (single and multi-configuration self-consistent fields, configuration interaction, pure and hybrid density functionals) and non-variational methods (perturbative Møller-Plesset and coupled-cluster methods for electron correlation). The treatment of magnetic effects in molecules has required the development of effective solutions to the "gauge problem", namely the dependence of the calculated properties on the choice of the origin for the vector potential **A** (where $\mathbf{B}=\nabla\times\mathbf{A}$, and $\nabla\cdot\mathbf{A}=0$ in the Coulomb gauge). Basically, a magnetic field introduces a complex phase in the electronic wave function, which in general will not be correctly reproduced when this is expanded in a finite (incomplete) basis set. The GIAO (Gauge-Including or Gauge-Invariant Atomic Orbitals [51,52]) and IGLO (Individual Gauges for Localized Orbitals[53]) methods currently represent the most effective and popular solutions to the problem, at least for molecular systems.

Over the last decade, in addition to further developments on very accurate predictions using correlated wave functions,[54] there has been an increasing emphasis on the application to larger, more complex systems, especially thanks to developments in Density Functional Theory (DFT, see refs. 55 and 56 for two entry points to a vast literature, including references for the density functionals which will be mentioned below) and linear scaling methods,[57-59] and in the treatment of environmental effects by implicit solvent or polarizable continuum models (PCM),[60,61] hybrid Quantum Mechanics / Molecular Mechanics (QM/MM) methods ,[62-64] or fully quantum mechanically by ab initio molecular dynamics with periodic boundary conditions.[65] Today, as a result of these efforts and developments, several computational packages allow the evaluation of chemical shifts (possibly also of other magnetic properties) by a variety of methods. A non-exhaustive list of "NMR-friendly" computational packages, which gives a feeling for the intense activity around this topic, includes Gaussian,[66] GAMESS,[67] NWChem,[68] ORCA,[69] Turbomole,[70] Jaguar,[71] Q-Chem,[72] Dalton,[73] CFOUR,[74] ADF,[75] CP2K,[76] Quantum Espresso[77] and CASTEP.[79] Gaussian's implementation of the GIAO method has somehow set the standard for general-purpose applications, but the other codes may offer superior performance either for small gas-phase molecules or for complex, condensed phase systems. The last codes on this list avoid the description of core electrons through the use of pseudopotentials. Because of this they cannot be used to compute absolute shielding constants, but they may still give good results for their relative values (i.e., the chemical shifts).[48]

On the front of accurate calculations on small molecules, Gauss' group has implemented chemical shift calculations for arbitrary coupled-cluster excitation levels (i.e., CCSDT, CCSDTQ and beyond).[79,80] Their results confirm the excellent performance of the less costly CCSD(T) method, whereby triple excitations from the Hartree-Fock (HF) reference wave function are treated perturbatively. For closed shell molecules with a good basis set (at least triple-zeta with polarization), this usually leads to errors within a few ppm's from the experimental absolute shielding constant. Reducing the error below 1-2%, if at all necessary, requires also the application of temperature-dependent vibrational corrections. Some illustrative results for the isotropic shielding constants of water, carbon monoxide and ozone are collected in Table 1. Water is a fairly simple molecule, at least in the gas phase (see below for the liquid phase). If we only consider convergence with respect to the electron correlation treatment, the results are virtually converged already at the CCSD level. Better agreement with experiment can be achieved by extending the basis set and, as a secondary effect, by vibrational averaging (see also ref. 81 for a systematic DFT study of the water molecule, including many density functionals and basis sets). Notice that convergence appears to be easier for ^{1}H than for ^{17}O. This will be a recurring theme, namely that the chemical shifts of ^{17}O appear to be more sensitive than those of other nuclei to "perturbations". We interpret this term in the broadest possible sense, including both real perturbations (e.g., non-bonded interactions interactions) and artificial ones (e.g., a change in the computational model, as in the previous

case). The description of the carbon monoxide shielding requires at least the CCSD(T) level, but for quantitative results the adoption of a large basis set is even more important than the inclusion of higher excitation levels. CO is an important molecule, also because it is the basis of the absolute shielding scale for ^{17}O (see below). Finally, ozone is a notoriously difficult molecule for NMR [41] and other spectroscopic properties, due to its biradical character which implies a substantial configuration mixing in the ground state (see ref. 82 and references therein). Indeed, a CCSD(T) description based on a closed-shell Hartree-Fock reference wave function leads to shielding constants for the terminal oxygens which are over 120 ppm's away from experiment. CCSDT is a clear improvement, but even this appears to be much farther from convergence than the other cases.

Table 1: Comparison of some isotropic shielding constants, calculated at the equilibrium geometries with different coupled-cluster methods (in ppm). FCI indicates the "exact" (for a given basis set) Full Configuration Interaction result. Unlike the calculated values, the experimental results include the effect of vibrational averaging.

	H_2O[a]		CO[a]		CO[b]		O_3[b]	
Nucleus	^{17}O	^{1}H	^{13}C	^{17}O	^{1}C	^{17}O	$^{17}O_{terminal}$	$^{17}O_{central}$
CCSD	335.24	31.822	32.23	-13.93	3.2	-52.0	-1402.7	-968.1
CCSD(T)	335.12	31.874	35.91	-13.03	7.9	-48.6	-1183.8	-724.2
CCSDT	354.99	31.879	35.66	-13.16	7.4	-49.0	-1261.1	-774.7
CCSDTQ	355.18	31.877	36.10	-12.81	-	-	-	-
FCI	355.18	31.877	35.15	-12.91	-	-	-	-
Exp. (300 K)	323.6[c,d]	30.05[d]	-	-	1.4[d]	-62.74[c]	-1310.5[c]	-744.5[c]

[a] Reference 79, cc-pVDZ basis.

[b] Reference 80, qz2p basis (11s7p2d/7s2p primitive set contracted to 6s4p2d/4s2p).

[c] Reference 83

[d] Reference 84

Another useful benchmark study was performed by Auer,[85] who compared accurate coupled-cluster and DFT calculations on methanol with recent gas-phase experimental data by Makulski[86] (see also ref. 87 for further DFT calculations). Some of his results are collected in Table 2. At the CCSD(T) level, we see that a major extension of the basis set produces a change of the order of 1.5 ppm for ^{17}O and ^{13}C, 0.5 ppm for ^{1}H. Further extensions to the basis set limit were estimated to change the result by less than 0.3 ppm, for ^{17}O. To achieve full agreement with experiment, it is much more important to include zero-point and temperature corrections. This involves the calculation of the derivatives of the chemical shifts with respect to the vibrational normal modes, calculated by second order vibrational perturbation

theory (see also ref. 88 for a study detailing the steps in the evaluation of the vibrational contributions to the chemical shifts of H_2O and other small molecules, by a somewhat different method). Both corrections are larger for ^{17}O than for ^{13}C, and eventually lead to a deviation with respect to experiment of 3.5 ppm for ^{17}O and 1.5 ppm for ^{13}C. As for the DFT calculations, which currently represent the only practical correlated methods for much larger systems, we notice that the PBE0 hybrid functional performs better than the others, but interestingly even this is not as good as a plain Hartree-Fock calculation on an isolated methanol molecule.

Table 2: Comparison of calculated[85] and experimental[86] gas-phase absolute shielding constants of methanol (in ppm). All calculations were carried out at the CCSD(T)/cc-pVQZ optimal geometry. Best estimate corresponds to the CCSD(T)/15s11p4d3f result with zero-point and temperature corrections.

Nucleus	^{17}O	^{13}C	$^{1}H_3C$	^{1}HO
CCSD(T)/qz2p[a]	342.80	143.17	28.435	32.292
CCSD(T)/15s11p4d3f	344.14	141.82	28.150	31.749
HF/15s11p4d3f	340.17	142.59	28.742	31.699
BP86/15s11p4d3f	322.46	124.55	27.893	32.141
B3LYP/15s11p4d3f	323.14	125.39	28.111	32.035
PBE0/15s11p4d3f	329.81	131.20	28.071	31.922
KT3/15s11p4d3f	317.29	130.37	28.098	32.247
Zero-point vib.	-11.97	-4.02	-0.701	-0.739
Temp. corr. (300 K)	1.29	0.00	-0.011	-0.065
Best estimate (300K)	333.46	137.80	27.438	30.945
Experiment (300 K)	329.9	136.46	27.313	30.631

[a] The qz2p basis corresponds to a 11s7p2d/7s2p Gaussian primitive set contracted to 6s4p2d/4s2p.

As mentioned above, an absolute magnetic shielding scale for oxygen was established by combining highly precise experimental measurements of the ^{17}O spin-rotation constant in carbon monoxide and accurate quantum chemical calculations of the diamagnetic contribution to this shielding.[83] The shielding constant for $^{12}C^{17}O$ was found to be -56.8 ppm at the equilibrium geometry, and -62.7 ppm after vibrational averaging at 300 K. On the same scale, appropriate for measurements at room temperature, the $H_2{}^{17}O$ shielding constants are 323.6 ppm in the gas phase and 287.5 ppm in the liquid phase. The latter represents the reference for many ^{17}O NMR experiments. The gas-phase $H_2{}^{17}O$ shielding constant is in excellent agreement with the vibrationally-corrected value which had been calculated earlier by Vaara et al.[89] (324 ppm).

The revised shielding scale[83] for ^{17}O has stimulated the measurement of an improved set of gas-phase shielding constants and gas-to-liquid shifts for over thirty oxygen-containing compounds.[84,90] The resulting compilation of gas-phase data represents an attractive testing ground for further ab initio calculations. The gas-to-liquid changes in the shielding constants,[90] defined as $\Delta\sigma_{GL}=\delta_{liq}-\delta_{gas}-4\pi\chi/3$ (where the δ's are chemical shifts with respect to an external liquid water sample and χ is the bulk magnetic susceptibility of the liquids), are an interesting manifestation of the effect of non-bonded interactions on the NMR spectrum (see the review on this topic by Bagno et al.[91]). For most compounds, this amounts to less than 10 ppm in absolute value, but for water it is $\Delta\sigma_{GL}$=-36.1 ppm (see above). Such a large shift clearly has to do with the strong perturbation produced by hydrogen bonding in the liquid phase. Notice, however, that methanol undergoes a much smaller shift ($\Delta\sigma_{GL}$=-8.3 ppm), while other non-hydrogen-bonding liquids have an unexpectedly large one ($\Delta\sigma_{GL}$= +24.3 ppm for acetaldehyde, +19.7 for acetone, -18.0 for F_2O).

Thanks to computational advances, nowadays it is common to describe the effect of solvation and other non-covalent interaction on the chemical shifts by performing large supramolecular calculations (i.e., including some explicit solvent molecules), often with the aid of QM/MM or continuum solvent models to describe longer-range effects from the environment. Some examples will be provided below. However, it should be borne in mind that many of these effects could also be described in terms of the perturbation by an electric field **F** produced by the surrounding molecules:[92]

$$\boldsymbol{\sigma}_K = \boldsymbol{\sigma}_K(0) + \frac{\partial \boldsymbol{\sigma}_K}{\partial \mathbf{F}} \cdot \mathbf{F} + \frac{\partial \boldsymbol{\sigma}_K}{\partial (\nabla \mathbf{F})} : (\nabla \mathbf{F}) + \ldots \qquad (23)$$

Here $\boldsymbol{\sigma}_K(0)$ is the shielding tensor of a nucleus within the unperturbed molecule, $\frac{\partial \boldsymbol{\sigma}_K}{\partial \mathbf{F}}$ is its dipole shielding polarizability and $\frac{\partial \boldsymbol{\sigma}_K}{\partial (\nabla \mathbf{F})}$ the quadrupole shielding polarizability (they are coupled to the field and the EFG at the nucleus, respectively). Subsequent terms in the series of Eq. (23) involve higher powers and higher derivatives of **F**. An early computational study of these quantities was carried out by Augspurger et al.[93] on a series of small molecules, with the aim to rationalize to origin of the chemical shift variations within a protein. In combination with an estimate of the typical electric field strengths generated by a protein's own charge distribution, they concluded that electrostatic effects could easily produce 10 ppm shifts for ^{17}O and 5 ppm shifts for ^{13}C. Again, notice the higher sensitivity of ^{17}O to external perturbations. One important motivation for that study was the need to improve the interpretation of ^{17}O NMR experiments on O_2 and CO bonded to the heme groups of oxygen-binding proteins[94,95] (see ref. 96 for subsequent ab initio DFT calculations of the ^{17}O chemical shifts and EFG's in related systems). Recently, it has been proposed the similar concepts could be used in order to assign a local dielectric constant to a protein's interior from the knowledge of its chemical shift perturbations.[97]

Going back to recent purely computational studies, the dipole[98] and quadrupole[99] shielding polarizabilities of several small molecules have been recalculated, respectively with coupled-cluster and Hartree-Fock wave functions. This approach has been applied to study the variation of the magnetic shieldings of N-methylacetamide upon solvation,[100] obtaining the shielding polarizabilities by gas-phase ab initio calculations and the electric field and its gradient by molecular dynamics simulations of this solute within a polarizable water model.

Recent computational work has addressed the effect of an applied electric field on the ^{17}O chemical shifts of complexes of peroxides (XOOX', X,X'=H,CH_3) with lithium cations.[101] This study was motivated by the theoretical possibility of discriminating enantiomers by NMR, by applying an electric field in the direction orthogonal to the static magnetic field.[102] The dipole shielding polarizability of a nucleus has a pseudoscalar component, which has opposite signs for two enantiomers. Therefore, different enantiomers should have slightly different chemical shifts in an electric field. Several complexes were investigated as candidate systems for the observation of this effect, but unfortunately the results indicate that an exceedingly high electric field (10^8 V/m) would be required to produce a 1 ppm shift between two enantiomers.[101] So far, this and analogous results on other systems has discouraged experimentalist from looking for this effect. However, Buckingham has recently pointed out that molecular polarity might enhance it significantly under appropriate experimental conditions.[103]

In the context of ^{17}O NMR spectroscopy, liquid water is important as the solvent for many experiments, as the reference for the chemical shifts of the other ^{17}O nuclei, and as a prototypical system for the study of the effect of intermolecular interactions on oxygen's NMR parameters. Thus, it is not surprising that the large shift experienced by $H_2{}^{17}O$ on going from the gas to the liquid phase has been the subject of several computational studies. An early calculation,[104] based on water's gas-phase dipole shielding polarizabilities (see above) in combination with molecular dynamics simulations, gave reasonable result for the proton chemical shift ($\delta(^1H)$=-3.86 ppm, versus the experimental value $\delta(^1H)$=-4.3 ppm at 300 K[105]), but failed completely for that of oxygen (calculated value $\delta(^{17}O)$=+4.34 ppm, versus the experimental value $\delta(^{17}O)$=-36.1 ppm at 300 K;[83] remember that the shifts describe the deviation of the gas-phase resonances from those in the liquid phase, which is taken as reference). A likely reason for this failure was the neglect of the effect of electric field gradients, since quadrupole polarizabilities could not be computed rigorously at the time. Another early calculation,[106] based on more straightforward (but more expensive) supramolecular calculations on water clusters extracted from a simulation, gave ^{17}O chemical shifts from -47 to -20 ppm, depending on the intermolecular potential employed in the simulations (all chemical shift calculations employed the so-called PW91 version of DFT). This pointed to the overall soundness of this computational approach, but the broadness of the chemical shift range demonstrated once more the high sensitivity of oxygen to subtle environmental effects. Pfommer et al.[107] were the first to use Car-Parrinello ab initio molecular dynamics[65] to generate

the atomic configuration and calculate the chemical shifts of both water and ice, on an equal footing (three-dimensional periodic boundary conditions, same plane-wave basis, same version of DFT). This calculation yielded a satisfactory -36.6 ppm for the gas-liquid shift (subsequently, an analogous calculation addressed also the supercritical state of water, but only for the ^{1}H chemical shifts[108]). A subsequent calculation by Pennanen et al.[109] combined the two approaches, by performing ab initio molecular dynamics simulations and extracting water clusters to carry out conventional all-electron quantum chemical calculations of the chemical shifts. A typical cluster had a roughly spherical shape and contained 15 water molecules. Longer-range electrostatic effects were represented by a reaction field (continuum dielectric outside the spherical cavity containing the cluster). The ^{17}O chemical shift calculated in this way were -24.3 ppm at the HF level and -41.2 ppm at the B3LYP level. In addition, the authors[108] evaluated the shielding anisotropies and EFG's, which are relevant for the interpretation of relaxation experiments. Finally, we mention that other authors have calculated the NMR parameters (chemical shifts and EFG's) of discrete water clusters, obtaining their structure from energy minimizations instead of molecular dynamics.[110-112] Such calculations have provided useful information on the relationship between the chemical shifts of individual oxygen and their local environment (extent and type of hydrogen-bonding, for example).

The calculations by Klein et al.[111] have also clearly highlighted the deficiencies of polarizable continuum models for ^{17}O NMR properties in a hydrogen bonding environment, as they predict the wrong sign for the $H_2{}^{17}O$ chemical shift when a single water molecule is surrounded by a continuum dielectric representing the bulk liquid. Similar observations were made by us in the ^{17}O NMR study of simple acids and peracids in aqueous solution.[113] On the other hand, while continuum models cannot replace the first solvation sphere, they may speed up appreciably the convergence of a calculation with respect to the surrounding solvent cluster size.[102,114-117] See also ref. 118 for problems and possible strategies to treat solvation in computational NMR.

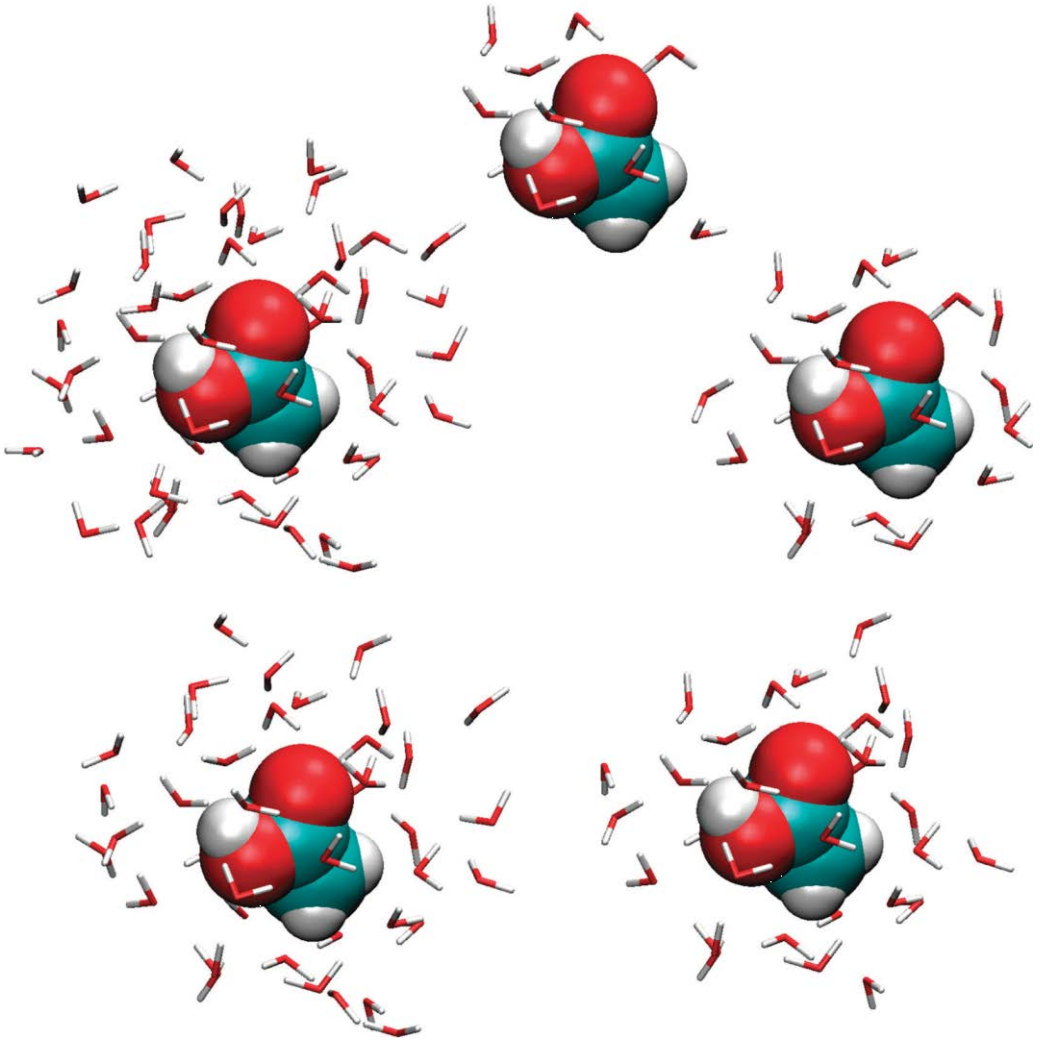

Figure 5: Representative configurations used in the calculation of the ^{17}O chemical shifts of acetic acid, solvated by (clockwise from the top) 10, 20, 30, 40 and 50 water molecules. Reproduced from ref. 117.

The success of the "molecular dynamics plus cluster" approach to the ^{17}O NMR spectrum of liquid water has encouraged the application of similar methods to study the solvation of other small oxygen-containing molecules. Calculations have been performed on aqueous solutions of dimethylether, formaldehyde and acetone,[114] *N*-methylacetamide,[115] acetone again,[116] hydrogen peroxide, acetic, lactic and peracetic acid,[117] uracil and 5-fluorouracil.[119] Many of these studies employed the PBE0 density functional with a reasonably sized Gaussian basis set (6-311+G(d,p), for example) for the calculations of the chemical shifts. The third one[116] included a calculation of the UV-VIS spectrum of acetone, in addition the ^{17}O NMR one, and demonstrated the importance of a careful reparametrization of the solute force field in order to obtain good spectroscopic properties. This can be a difficult and lengthy task, especially for larger solutes. A possible alternative is to perform a full ab initio molecular dynamics simulation,[65] but this requires considerable computational resources. In our own work,[117] we have

employed a QM/MM approach,[64] describing water with a conventional force field and the solute with the semiempirical PM6 method,[120] which had been parametrized by Stewart with the explicit aim of improving the description of hydrogen bonds. This strategy avoids the force field parametrization step, at the cost of a modest increase in computer time. The best results (within an average of 9 ppm from the experimental peaks, which is satisfactory as it is comparable to their widths) were obtained by a) including about thirty explicit water molecules in the chemical shift calculations, b) embedding this solute-solvent cluster within a polarizable continuum and c) performing a couple of DFT minimization steps on each cluster before the chemical shift calculation, instead of using configurations coming directly out of the molecular dynamics simulation (see Figure 5). The partial minimization step corrects small but systematic "imperfections" in the solvent configurations, presumably due to the use of a standard, non-polarizable water force field. In the specific case of peracetic acid ($CH_3(CO)OOH$), the two calculated peaks associated with the peroxidic oxygens are almost 40 ppm apart within an implicit solvent, but they come within 7 ppm of each other after explicit solvation. The latter is consistent with the observation of only two peaks in the experimental spectrum (one for the carbonyl oxygen, one for the two peroxidic ones). Thus, explicit solvation is essential in order to arrive at a proper interpretation of the experimental spectrum.[113]

Before leaving the subject of intermolecular effects on ^{17}O chemical shifts, we mention that some authors have analyzed the correlation between their values and the topological properties of the molecular electron density,[121] respectively in water clusters[111] and in dichloroacetic acid aggregates.[122] Another recent study has addressed the calculation of the NMR parameters of water chlatrate models incorporating carbon dioxide, in order to identify some spectroscopic signatures of their presence and structure.[123]

A possible strategy for cutting down the cost of chemical shift calculations on large molecules, which is alternative to the QM/MM approach, is to retain a full QM description, but simplifying it by partitioning the molecule into fragments.[124] In the combined fragmentation method (CFM), capping hydrogens are placed to satisfy the valency at broken bonds, and the total energy is obtained as the sum of a first order estimate corresponding to the sum of the energies of the individual fragments, and a correction accounting for all pairwise interactions among them (the form of the correction depends on whether the two fragments are covalently linked or not). The method has been applied to the calculation of the chemical shifts of several small proteins, typically containing 100-150 atoms.[125] The chemical shift calculated by the CFM were compared to those from conventional calculations on the whole proteins, at the same level of theory (HF with a 6-311G* basis set, within a polarizable continuum solvent). In the first-order version of the CFM, without nonbonded interactions among the fragments, the root-mean-square errors were 0.340, 0.649, 3.052, 6.928 and 0.122 ppm, respectively for ^{1}H, ^{13}C, ^{15}N, ^{17}O and ^{33}S. Including the effect of nonbonded interactions reduced these error to 0.038, 0.252, 0.681, 3.480 and

0.052 ppm, respectively. The authors point out that the result for ^{17}O is in line with those of the other nuclei, when one expresses the error as a percentage of its chemical shift range (2.62%). Even so, this demonstrates once more the sensitivity of ^{17}O to the details of the surrounding environment.

Since ^{17}O is so sensitive to intermolecular interactions, it is not surprising that conformational effects can be large too. This has been demonstrated, for example, by a series of calculations on α,β-unsaturated ketones and esters.[126] The chemical shifts of different conformations of these compounds may be up to 100 ppm apart. In principle, this allows the study of the conformational preference of these and similar systems by ^{17}O NMR spectroscopy.[127] The same group has also used a combination of ^{17}O NMR spectra and DFT calculations to describe the structure and the fluxional behaviour of organic reactants based on iodine bonded to carboxylate groups.[128,129] These represent interesting examples of the modern approach to the interpretation of the ^{17}O NMR spectra of complex organic compounds, exploiting the possibilities offered by current ab initio methods.

The calculation of the ^{17}O chemical shifts has also been applied to problems in inorganic chemistry. One recent example involving main group elements concerns the interpretation of the temperature dependence of the ^{17}O and ^{33}S spectra of liquid SO_3.[130] These could be assigned on the basis of the equilibrium between the monomer and the cyclic trimer $(SO_3)_3$, excluding substantial amounts of other multimeric forms. Another study has addressed the calculation of the NMR parameters of ^{29}Si and ^{17}O (chemical shifts tensors and also the EFG ones, for the latter) in the main crystalline silica polymorphs (α-quartz, α-cristobalite, coesite, Sigma-2 and ferrierite zeolites).[131] The calculations were performed by cutting out cluster models of increasing size (up to 130 atoms, using hydrogens to cap dangling bonds), and involved also the comparison of HF and several DFT methods. The authors achieved full convergence with respect to the cluster size for ^{29}Si, while for ^{17}O this was not possible and a QM/MM description based on partial atomic charges representing far away atoms had to be adopted, with mixed results. Also, the HF method proved fully adequate for ^{29}Si, while the DFT methods performed marginally better for ^{17}O (average errors on the relative chemical shifts of different oxygen sites were 5.7, 4.5, 4.4, 4.7, and 3.9 ppm for HF, B3LYP, PBE0, M05-2X, and PBE methods, respectively). Once more, we note the high sensitivity of the ^{17}O resonances to subtle perturbations.

Several studies have applied ^{17}O NMR to the chemistry of transition metals and their coordination complexes. One of them, on aqueous Ni(II), has already been mentioned in Section 2.4 on paramagnetic relaxation.[39] Some others will be discussed below, in the context of their application as paramagnetic contrast agents for MRI. Here me mention a few purely computational studies on multi-nuclear clusters and polyoxometalate cages.[132-134] The last one of these contains an extensive series of calculations on the effect of different basis sets, density functionals and geometry optimizations on ^{17}O chemical shifts in polyoxometalates cages derived from the $[W_6O_{19}]^{2-}$ anion, which may be of interest to those approaching this type of calculations.[134] Note that, in the presence of heavy elements such as W,

relativistic effects (i.e., spin-orbit coupling) become important and they have to be properly accounted for. The calculations can easily discriminate the chemical shifts of the terminal (oxo), bridging and central oxygens, as they span 1200 ppm. Changing W(+6) with another metal cation, or changing their oxidation states, produces systematic variations in the shielding constants of the oxygens bonded to them. According to the same study, the ^{17}O chemical shifts can also be used to identify the protonation sites of these clusters, at low pH.

3.2 Spin-spin coupling constants

The calculation of the indirect, through-bond or scalar *J*-couplings has been discussed in a few reviews.[41,135,136] Like the shielding constants, also these can be expressed as derivatives of the total energy of a molecule:

$$\mathbf{K}_{KL} = \left.\frac{\partial^2 E}{\partial \mathbf{M}_K \partial \mathbf{M}_L}\right|_{\mathbf{B}=0,\mathbf{M}_{J\neq K,L}=0} - \mathbf{D}_{KL} \qquad (24)$$

where $\mathbf{D}_{KL}$ the direct dipolar coupling tensor.[13-16] There are important differences between the chemical shifts and the indirect couplings, which may not be apparent from Eqs. (22) and (24). First of all, while $\boldsymbol{\sigma}_K$ can be calculated from the response of the electron distribution to the three components of **B**, without knowledge of the response to the magnetic moments of the individual nuclei, $\mathbf{K}_{KL}$ explicitly requires them. The final equations are more involved and they have been incorporated in a smaller number of codes, as compared with those allowing the calculation of chemical shifts. Secondly, while Hartree-Fock theory provides a useful starting point for the calculation of the chemical shifts in closed-shell molecules, it is almost useless for the spin-spin couplings, especially those across multiple bonds, where a balanced description of electron correlation effects is mandatory. Finally, since the *J*-couplings are usually dominated by the Fermi contact contribution and this requires an accurate description of the electron density at the nuclei, it may be necessary to adopt non-standard basis sets with very high orbital exponents for the *s*-type Gaussian functions. For all of these reasons, the calculation of the indirect couplings is a much heavier and less standardized task, especially for molecules with many nuclei. The Gaussian,[66] NWChem,[68] Dalton,[73] CFOUR,[74] ADF[75] and CASTEP[78] codes allow the calculation of these indirect spin-spin couplings, with different degrees of approximation.

There are only a few calculations of *J*-couplings involving ^{17}O. The reason is that multiplet structures are usually unobservable in ^{17}O NMR spectra of liquids, due to the breadth of the resonance peaks. However, this becomes possible under special circumstances, as demonstrated by the recent observation of $^4J(^{19}\text{F},^{17}\text{O})$ couplings in some fluorine-substituted phenylboronic acids, with values of the order of 25 Hz.[137] One theoretical paper specifically devoted to such calculations is due to Bryce,[138] who computed the *J*-coupling between ^{31}P, ^{27}Al and ^{17}O in small molecules and cluster. These were constructed as models of aluminophosphate and grossite minerals, and included also triphenylphosphine

oxide. The author reports $^{1}J(^{27}Al,^{17}O)$ and $^{1}J(^{31}P,^{17}O)$ values, computed with the B3LYP hybrid density functional and several basis sets. Also Siuda and Sadlej[123] have used the B3LYP functional to compute both intramolecular and intermolecular coupling constants involving ^{17}O, in their models of CO_2 embedded in water cages (chlatrates). Their results suggest that, together with the ^{13}C and ^{17}O chemical shifts, the $^{1}J(^{13}C,^{17}O)$ coupling in CO_2 could also be used to discriminate between chatrated and gaseous molecules.

3.3 Electric field gradients

As mentioned earlier in connection with Figure 3, there is a good degree of transferability in the quadrupolar coupling constants (C_q) and therefore also in the principal components of the EGF tensor around ^{17}O, when this is found different bonding environments. Autschbach et al.[139] have authored a useful introduction to this topic. Using ab initio calculations in combination with simple point-charge models, they arrive at a qualitative, chemically appealing rationalization of origin of these parameters (sign, values and orientation of the EFG with respect to the local molecular frame). In the same paper, they also present several DFT calculations of the EFG for several small and medium-size molecules, including also transition metal complexes. In the same spirit of the high-level benchmark calculations of the shielding constants in small molecules, Brown and Wasylishen[140] have carried out carried out a detailed experimental and computational study of the nuclear quadrupole coupling constants in N_2O. Their calculations include several types of correlated calculations ─ CCSD(T) and multi-reference configuration interaction, for example ─ with large correlation-consistent basis sets. A simple additional calculation on a linear FH…NNO complex demonstrates a large change in the EFG at the terminal nitrogen, showing that intermolecular effects can also be important after all. Both papers[139,140] are recommended to anyone looking for guidelines on the quantitative performance of different methods.

Turning to specific applications in ^{17}O NMR, we may mention the EFG calculations on CO-heme model compounds,[96] liquid water,[109] water clusters,[112] and the silicon dioxide polymorphs.[131] Sebastiani and coworkers[141] have performed “on the fly” calculations of the EFG within an ab initio molecular dynamics simulation of liquid water. We will return to this paper in Section 6, which is devoted to relaxation studies. Finally, we mention a detailed analysis of the effect hydrogen- and halogen-bonding interactions on the EFG’s of chloroacetic acid.[142]

4. Applications of ^{17}O NMR in chemistry and materials

In the first of his two reviews,[2] Gerothanassis has devoted about fifty pages to a systematic description of the chemical shifts of oxygen bonded to different elements, essentially covering the whole

periodic table. The reader seeking information on specific systems is encouraged to start from that review and, for organic compounds, the handbook edited by Boykin.[1] In this section we provide some recent examples of the use of ^{17}O NMR spectroscopy for the elucidation of reaction mechanisms, for structural studies and as a probe of molecular interactions in liquids.

Substituent effects and organic reaction mechanisms. Brownlee and co-workers published a milestone collection of NMR chemical shift data aimed at monitoring the electronic effect of substituents on aromatic compounds via conjugative and inductive effects.[143] Their approach was mainly based on the use of ^{13}C chemical shift at selected sites of 1,4-disubstituited aromatic compounds for linear free energy relationships. The systematic exploitation of ^{17}O NMR data to derive Hammet-type relationships describing the transmission of the electronic effects of substituents in many classes of aromatic compounds was started by the groups of Boykin[144] and Exner.[145] More recently, Maccagno et al.[146] have reported on the ^{17}O NMR substituent chemical shift of the carbonyl and methoxy oxygen atoms in a collection of sterically hindered 2,6-dimethyl-4-X-benzoates. The comparison of these data with the ones from the analogous compounds without the methyl substituents has shown that ^{17}O chemical shifts are extremely sensitive to the steric effects experienced by the oxygen atoms. Nummert et al. have examined 35 *ortho*-, *para*- and *meta*-substituted phenyl tosilates.[147] The ^{17}O NMR chemical shifts at the sulphonyl ($-SO_2-$) and at the single bonded phenoxy (-OPh) groups have been used as input for a dual substituent parameter regression analysis. Substituent effects and free energy relationships for a large collection of 1,3,4-oxadiazoles have also been reported by Gierczyc et al. on the basis of ^{17}O chemical shift data.[148]

Further work on substituent effects, using computed instead of experimental chemical shifts on a series of benzaldehydes, has been described by Kiralj and Ferreira.[149] Due to electron delocalization, the introduction of substituents can sometimes produce surprising long-range effects (i.e., across several bonds) on the ^{17}O chemical shifts, as demonstrated by a combined experimental-computational study of several monoaminoxidase inhibitors by Cerioni et al.[150].

The ^{17}O chemical shift of a large repertoire of organic compounds containing B-O bonds have been reported. In particular, the influence of the substituents present in the phenyl ring of phenylboronic acids and their derivatives on the ^{17}O chemical shift have been investigated.[151,152] The largest changes of ^{17}O shifts were observed for the *ortho* position. The effect of intermolecular hydrogen bond formation in the boronic acids also has been detected by ^{17}O chemical shift changes.[153]

As mentioned in the introduction to this Section, ^{17}O NMR chemical shift data can be an important investigating tool for mechanistic and structural problems. This point has been recently underlined in an important review dealing with the synthesis, structural characterization and reactivity of hydrogen trioxide HOOOH.[154] The ^{17}O spectrum, reported in Figure 6, shows two lines for the two magnetically non-equivalent oxygen atoms.[155] As expected, a significant deshielding of the oxygen nucleus is observed on going from $H^{17}OH$, to $H^{17}OOH$ (at 187 ppm), to $H^{17}OOOH$ (at 305 ppm), and

finally to HO[17]OOH (at 421 ppm). The observed chemical shifts were also fully confirmed by CCSD(T) calculations. The presence of hydrotrioxydes as actual reaction intermediates in the ozonation of aldehydes has been unambiguously demonstrated also with the aid of ^{17}O NMR data.[156]

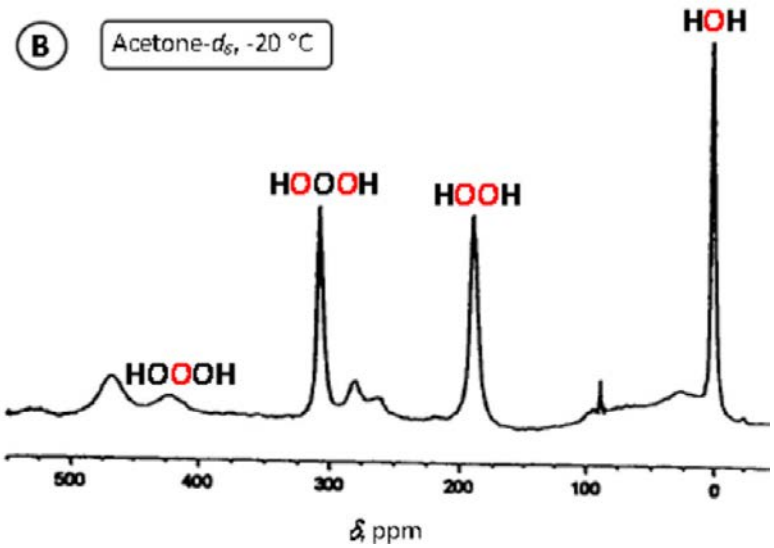

Figure 6. ^{17}O NMR spectra of HOOOH obtained by low-temperature ozonation of 1,2-diphenylhydrazine. Reproduced from ref. 155.

Sophisticated applications of ^{17}O NMR spectroscopy for the elucidation of reaction mechanisms have been reported. For example, the mechanism of the McKenna reaction – an important route for the synthesis of organophosphorous acids – has been assessed by the use of isotopically enriched diethyl phosphonates reagents containing P=^{17}O and P=^{18}O moieties.[157] The combined use of ^{31}P and ^{17}O NMR spectroscopy allowed to trace the fate of the O atom in the course of the reaction (^{18}O produces a slight, bond-order dependent shift in the resonance of a ^{31}P atom directly bonded to it).

Heavy transition metals. ^{17}O NMR has been applied to study oxygen bound to heavy transition metals. A brief review[158] of the properties of the AnO_2 cubic oxides (where An indicates the actinides U, Np, Pu and Am) discusses recent insights obtained by solid-state NMR studies of ^{17}O and other nuclei. Uranyl species in aqueous solutions containing H_2O_2 have received a lot of attention in connection with the disposal of spent nuclear fuels. Several studies have addressed the dissolution behaviour of uranyl ions (UO_2^{2+}) in solutions containing H_2O_2 and carbonate ions, which exist under geological disposal conditions.[159] Remarkably sharp ^{17}O resonance for the uranyl oxygen within the $UO_2(CO_3)_3^{4-}$ complex has been observed at 1099 ppm. Increasing the H_2O_2 concentration, the intensity of this peak decreases and two new peaks appear at 1094 and 1103 ppm, respectively attributed to the formation of $UO_2(O_2)(CO_3)_2^{4-}$ and $(UO_2)(O_2)(CO_3)_4^{6-}$complexes. Zanonato et al.[160] have identified several uranyl-peroxide-carbonate complexes in solution, proposed models of their structure and determined the values

of their equilibrium formation constants. Moreover, the solubility and the intermolecular interaction of several uranyl and vanadyl complexes with CO_2 have been investigated in supercritical carbon dioxide,[161] using an NMR spectrometer equipped with a high pressure cell.

Szabo et al.[162] have studied the formation and the structure of uranium complexes with four nucleotides, adenosine (AMP), guanosine (GMP), uridine (UMP), and cytidine-monophosphate (CMP) at alkaline pH (8.5-12) by multinuclear NMR spectroscopy, providing all spectral parameters and the diffusion coefficient data. Two complexes are formed with all ligands in the investigated pH region, independently of the total uranium(VI) and ligand concentrations. The uranium-to-nucleotide ratio is 6:4 in one of the complexes and 3:3 in the other one.

Relativistic density functional theory was used to calculate structural data such as bond lengths, vibrational frequencies and ^{17}O NMR chemical shifts for the $[NpO_2(OH)_4]^{1-}$ and $[NpO_4(OH)_2]^{3-}$ complexes, which correspond to different hydration states of Np(VII) in alkaline solutions.[163] The calculations prove that the latter predominates and that both complexes have stronger bonds than their formally isoelectronic uranium(VI) analogues. The experimentally observed 300 ppm difference between the chemical shifts of ^{17}O bonded to Np(VII) and to U(VI) was shown to be mainly a function of the central metal and not of the coordination environment or protonation state.

Neoteric solvents. The environmental issues of chemical manufacturing and the increased sensitivity of the chemistry community to the "green" aspects of research have stimulated a growing interest towards unconventional, environmentally benign solvents, commonly referred to as "neoteric solvents". In this context, the innovative use of water as reaction medium for organic reaction, as well as the use of supercritical water and CO_2, deserve to be cited. Beyond these, two other important classes of new solvents have gained popularity starting from the '90s: ionic liquids and organic carbonates.

Ionic liquids are low-melting salts ─ m.p. generally below 100 °C ─ commonly formed by a bulky organic cation (tetralkylammonium, pyridinium, imidazolium, pyrrolidinium, etc.) and an often inorganic, polarizable, fluorine-containing anion (PF_6^-, BF_4^-, $[(CF_3SO_2)_2N]^-$, acetate, triflate, etc.). The consequent "packing frustration" prevents the organization of the ions in a crystal lattice, thus leading to isotropic liquids instead of crystalline solids. The chemistry and physical chemistry of these systems is the object of a large scientific production and will not be summarized here. The interested readers may refer to the recent review by Weingärtner.[164]

The so-called "first generation" ionic liquids consisted of a mixture of organic salts and chloroaluminates. Seminal papers in this field contain useful and elegant applications of ^{17}O NMR in elucidating the chemistry of water in these systems. Zawodzinski and Osteryoung identified the by-products formed by water in mixtures of imidazolium chlorides and $AlCl_3$.[165] The group of Seddon provided clear-cut validation of a general method for oxide contaminants removal from imidazolium/$AlCl_3$ ionic liquids by ^{17}O NMR in the presence of water traces.[166]

Chloroaluminate-based ionic liquids have been abandoned in the last two decades, having been replaced with single components systems. The recent literature on the subject contains some limited, niche applications of ^{17}O NMR. Xu et al.[167] have studied innovative components for energy storage devices. Their Na–CO_2/O_2 battery included a small amount of imidazolium-based ionic liquid to improve the performance in terms of high-voltage stability. The absence of water, a critical factor for correct operation, has been demonstrated by a thorough analysis of the ^{17}O NMR spectra. ^{17}O NMR spectroscopy has also been used to study the ligand-exchange rates of lanthanide ions in 1-ethyl-3-methylimidazolium ethyl sulfate.[168] The results have been compared to the analogous data in aqueous environment. The observed exchange rates show a marked dependence on the solvent composition. These results open the way to tuning the ligand-exchange rate, with interesting perspectives for the separation of lanthanide ions.

As mentioned above, organic carbonates are an important class of innovative solvents recently considered for several applications. A remarkable example is provided by the work of Greenbaum, Xu and coworkers in the field of energy-storage devices, specifically lithium ion batteries.[169] Several mixtures of ethylene carbonate (EC), dimethyl carbonate (DMC) and 1M $LiPF_6$ have been studied as model systems, to understand lithium-ion solvation and transport in these liquids. The lithium salt produces shifts in the ^{17}O NMR peaks of the carbonates, which are largest for EC's carbonyl groups. Thus the spectra provide clear evidence for the preferential interaction of the Li^+ ions with these groups, rather than with the ethereal oxygens and with DMC. The data also furnish a more detailed picture of the Li^+ solvation shell, by the quantification of the average number of EC and DMC molecules interacting with it at every composition.

Gels. Important structural details about the formation of hydrogels of polysaccharides in the presence of suitable electrolytes have been obtained by ^{17}O NMR. Dextran gels have been studied by Chen et al.[170] by chemical shift and line-width analysis of the ^{17}O NMR signals as a function of the amount of added KCl. The selective broadening of hemiacetalic oxygen atoms of the polysaccharide backbone have confirmed the KCl binding mode and shed light on the role played by the salt in the physical cross-linking process leading to the hydrogel.

5. Applications of ^{17}O NMR in biology

The first applications of solution ^{17}O NMR spectroscopy in biology concern the study of protein-ligand interactions using ^{17}O-labeled small molecules, such as $^{17}O_2$ and $C^{17}O$ (but also ^{13}CO) bound to ferrous heme proteins.[94,95,171] The ^{17}O spectral parameters, chemical shifts, nuclear quadrupolar coupling constant and rotational correlation times τ_c were determined from line shape and relaxation data analysis. Sharp lines are observed (Figure 7.a)) for the CO ligand bound to large macromolecules in aqueous solution.

Since the tumbling motion of large biological molecules in solution is nearly always in the slow motion limit ($\omega_0\tau_c >> 1$), this leads to a multiexponential relaxation of the Quadrupolar Central Transition (QCT, see Section 2.3). For three ^{17}O-labeled ligands such as palmitic acid, oxalate and biotin bound to model proteins of size ranging from 65 to 240 kDa, the ^{17}O QCT high resolution NMR spectra were acquired and used to probe the molecular environment around the oxygen atoms.[172] Figure 7.b) shows the ^{17}O QCT NMR spectra of a ternary complex consisting of ovotransferrin (OTf), Al^{3+} and [$^{17}O_4$]oxalate in aqueous solution.[21] It is important to observe that, in presence of excessive oxalate ligands, both free and protein-bound oxalates were observed in the ^{17}O NMR spectra.

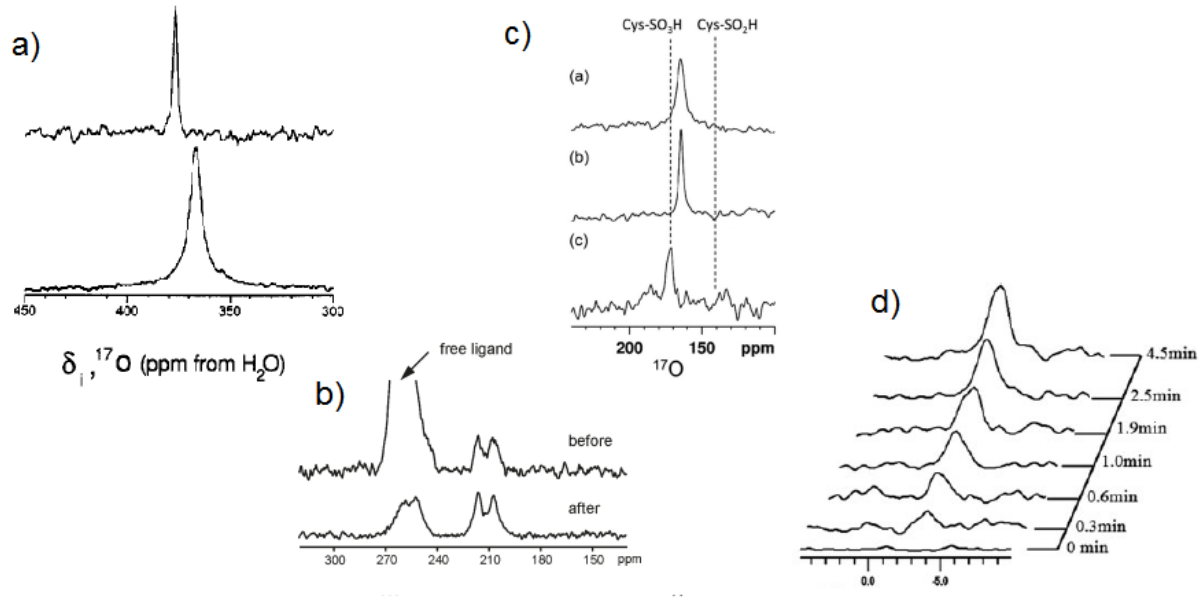

Figure 7. Representative ^{17}O NMR spectra of: a) CO-heme systems, from ref. 171, b) OTf-Al-[$^{17}O_4$] oxalate complex, from ref. 21, c) different forms of the SOD1 protein, from ref. 173, and d) mitochondrial $H_2{}^{17}O$ at variable times, from ref. 174.

The first example of a solution NMR study of ^{17}O-labeled proteins has been reported in a recent paper by Hanashima et al.[173]. The work focuses on the structure and dynamics of the human Cu,Zn-superoxide dismutase (SOD1), a homodimeric protein composed of 16 kDa subunits, whose role is to protect the cell from the oxidative aggression of the superoxide anion (O_2^-) by converting it to hydrogen peroxide. This occurs by oxidation of the –SH group of the Cys^{111} side chain, which is selectively converted to $–SO_3H$ or to $–SO_2H$. These positions were labelled using $^{17}O_2$ as an oxidant and the spectra recorded. Figure 7.c) shows the resulting ^{17}O NMR spectra of (from top to bottom) the so-called Cu^{2+}-form and Cu^+-form of SOD1, and that from a control experiment in which the protein was digested by

treatment with a peptidase. The clear differences in the ^{17}O spectra of the two forms suggest environmental, structural and dynamic differences among them.

A recent application of ^{17}O high resolution NMR in medicine concerns the study of heart metabolism by observing the metabolically produced $H_2{}^{17}O$ in isolated rat hearts. [174] These were perfused with $^{17}O_2$-enriched Krebs-Henseleit buffer with different Ca^{2+} concentration. Dynamic ^{17}O NMR spectra (Figure 7.d)) showed a progressive increase in the $H_2{}^{17}O$ resonance peak, thus indicating the production of mitochondrial $H_2{}^{17}O$. The peak intensity was used to evaluate the myocardial $^{17}O_2$ consumption rate.

Recently Prasad et al.[175] reported the first description of the reaction mechanism catalyzed by cytochrome $P450_{cam}$, a bacterial monooxygenase. At low O_2 concentration, this enzyme oxidizes water to H_2O_2 and simultaneously reduces camphor to borneol. ^{17}O NMR spectra were used to follow the H_2O_2 production and to confirm the proposed mechanism.

6. Relaxation studies

As mentioned in Section 2, relaxation is a wide-ranging phenomenon which may manifest itself in different ways and, in one way or another, affects every NMR experiment. In the following, we have separated the discussion of ^{17}O NMR relaxation in two parts. The first one concerns the dynamics of water, either pure or in presence of proteins or nanoparticles. In this case relaxation is dominated by quadrupolar interactions (see Section 2.3). The second one concerns relaxation in presence of paramagnetic complexes (see Section 2.4), which is important both in inorganic chemistry and in MRI.

6.1 Water and proteins

Water is obviously the most important liquid. Its structure and dynamics has been studied by virtually every possible method, including ^{17}O NMR. The large shift in the $H_2{}^{17}O$ signal on going from the gas to the liquid phase depends on the formation of a disordered, hydrogen-bonded network and it has been successfully reproduced by a combination of molecular dynamics and quantum chemical calculations (see Section 3.1). Sebastiani and coworkers[141] have carried this approach one step forward, by using Car-Parrinello ab initio molecular dynamics simulations to describe spin relaxation of the quadrupolar nuclei in liquid water (both ^{17}O and ^{2}H). Their simulations are relatively standard (64 water molecules in a cubic box with periodic boundary conditions, BLYP density functional), except for the fact every 2 fs they compute the EFG at all nuclei from the instantaneous atomic coordinates and electron density. Their average coupling constants are $\langle C_q \rangle = 7.9$ MHz for ^{17}O and 229 kHz for ^{2}H, in excellent agreement with the experimental values (7.7 MHz and 230 kHz, respectively). Furthermore, they derive the longitudinal relaxation rates from the time-correlation functions of the EGF's. Their T_1 values are

2.3 ms for ^{17}O and 0.23 s for ^{2}H, also in good agreement with experiment (6.6 ms and 0.7 s, respectively). It is remarkable that both relaxation times can be predicted so well, even though they are much longer than the overall simulation time (35 ps). Notice that this calculation avoids the assumptions of an intramolecular EFG and of an exponential decay of the correlation functions.

The dynamics of water in the supercooled state (down to -37 °C) has been investigated by Qvist et al. [178] through accurate measurements of the T_1 relaxation times in $H_2{}^{17}O$ (and D_2O), using isotopically enriched samples. The key scientific issue behind this work is the origin of the strong super-Arrhenius behaviour of the rotational correlation time and other transport properties (i.e., their activation energies appears to increase on lowering the temperature). With the aid of classical molecular dynamics simulations, the authors interpreted it in terms of discrete orientational jumps of the molecules with a non-exponential distribution of waiting times, which is a signature of dynamical heterogeneity (i.e., the presence of water regions with different mobilities).

The group of Halle has also reported extensively on water dynamics in protein solutions. Unlike the other relaxation studies discussed in this review, which employ high-resolution NMR, these were performed by Magnetic Resonance Dispersion experiments (MRD, see ref. 177 for an introduction). These involve measurements of the longitudinal relaxation rates of $H_2{}^{17}O$ (and D_2O) as a function of the Larmor frequency, which is controlled by changing the applied magnetic field. The resulting dispersion profiles (i.e., the functions $R_1(\omega_0)$) can be used to discriminate among water molecules with different dynamics, due to their interaction with the protein. The borderline between “free” and “associated” water molecules may be conventionally set at a residence time of 1 ns.[177] The experiments can be repeated at different temperatures, to change the relative amounts of each type. The technique has been used to study water at the outer surfaces (hydration layer)[177,178] and within the inner pockets of proteins (“buried” and “crystallographic” water).[179-181] Finally, we mention that ^{17}O NMR line width has also been used to study the effect of dispersed nano-materials on the dynamics of water.[182]

6.2 Paramagnetic complexes and MRI contrast agents

The relaxation of the $H_2{}^{17}O$ signal at high fields is enhanced by the presence of paramagnetic complexes and this can be exploited both for fundamental coordination chemistry studies and in the development of new contrast agents (CA) for MRI. The first example of a modern MRI CA is the gadolinium(III) complex of DTPA (diethylenetriaminepentaacetic acid, see Figure 8.a) for its chemical structure), approved for clinical use in1988.[183,184] Following this, several complexes with acyclic and macrociclic ligands have been proposed[185,186] with the aim of

producing CA's with enhanced relaxivity (a CA with a higher relaxivity produces the same effect in smaller doses, with obvious benefits for the patient undergoing an MRI scan).

According to the established model of paramagnetic relaxation (SBM theory, see Section 2.4), the number *(b)* and residence lifetime (τ_M) of the metal-coordinated water molecules, and the rotational motion of the paramagnetic system (τ_R) are the key parameters to be optimized in order to increase the relaxivity.[187] Typical values for CA's in current use are: one coordinated water molecule, more than 100 ns for τ_M and 0.1 ns for τ_R.[188] The synthesis of ligands capable of forming stable lanthanide complexes with two or more water molecules bound in the first (inner) coordination sphere ($b \geq 2$) has been pursued for a long time.[189] Here the difficulty is to increase the hydration state of the metal ion by reducing the number of donor atoms of the chelator, without compromising the thermodynamic and kinetic stability of the complex. The solution structure, stability and dynamics of several lanthanide complexes have been extensively studied using high resolution ^{17}O relaxation.[190-192] Complexes with other metal ions such as Mn(II) have also been proposed and characterized.[193,194] The design of new complexes has relied also on DFT calculations of chemical shifts and of hyperfine coupling constants, which are responsible for the scalar contribution to the oxygen relaxation rates.[195,196]

An interesting study of lanthanide-DTPA complexes in solution has been reported by Fusaro et al.[197]. Unlike the previous studies, where the ^{17}O NMR experiments essentially follow the dynamics of the water molecules, this was aimed at characterizing the structure and internal dynamics of the complexes using ^{17}O-enriched DTPA. A series of both diamagnetic and paramagnetic ions has been considered and the ^{17}O NMR spectra of the Ln-DTPA chelates have been acquired over a wide range of temperature. The signal line width has been used to calculate the activation energy of the dynamic process. Representative NMR spectra are reported in Figure 8. Similarly, ^{17}O NMR studies at variable temperature have been performed by Mayer et al.[198] to determine the activation energy of dynamic rotation processes taking place in the coordination complexes of lanthanide metal ions.

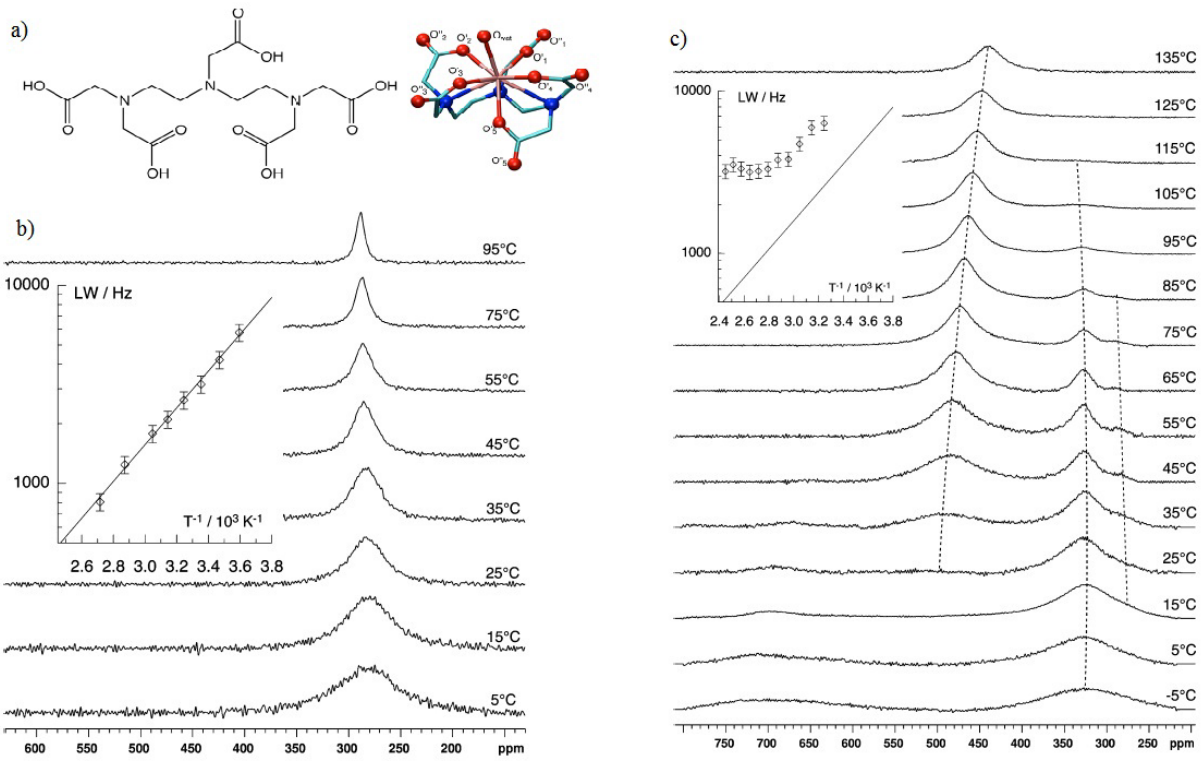

Figure 8: a) Chemical structure of the DTPA ligand, b) ^{17}O NMR spectra of La-DTPA complex at variable temperature, c) ^{17}O NMR spectra of Pr-DTPA complex at variable temperature. Adapted from ref. 197.

Paramagnetic effects on the relaxation rate and chemical shift differences between free (bulk) and metal-bound $H_2{}^{17}O$ enable the study of water exchange mechanisms in transition metal complexes. Water exchange reactions are usually fast enough to produce a broadening of the bound water resonance in the ^{17}O NMR spectrum, but slow enough to give two well resolved ^{17}O NMR signals corresponding to bound and free water. Nearly all water exchange rate constants on metal ions have been measured by NMR, mostly as a function of temperature to elucidate the mechanism of the reaction.[199] The use of special equipment allowing the application of high pressures offers an additional opportunity to discriminate among different mechanisms.[5]

A review of ligand exchange and complex formation reactions for *fac*-$[(CO)_3M(H_2O)_3]^+$ (M = Mn(I), Tc(I), Re(I)) and *fac*-$[(CO)_2(NO)Re(H_2O)_3]^{2+}$ complexes, as studied by oxygen NMR relaxation, is available in the literature.[200] These systems are important as precursors for a variety of radiopharmaceuticals which are under development. The water exchange kinetics for several metal complexes with chelating ligands $[M(L)(H_2O)]^{2-}$ (M=Mn(II), Fe(II), Ni(II) and L=edta, tmdta) has also been investigated.[201] The results indicate that, for the investigated divalent metal centers, the kinetic parameters are controlled by the *d*-orbital occupancy and by

the ligand architecture. The Mn(III)-porphyrin[202] complexes are important due to the involvement of the Mn(III) center in the enzymatic catalysis of redox reactions, such as superoxide dismutation (SOD). ^{17}O NMR relaxation experiments have shown that water exchange rates are very high and almost identical to the corresponding rate in $[Mn(H_2O)_6]^{2+}$.[203] The high lability of the axially bound water has been explained in terms of the *cis*-effect of porphyrin ligands and the Jahn-Teller distortion in the d^4 high-spin electronic configuration of Mn(III).

7. Conclusions

In the title of this review, we have called ^{17}O NMR a "rare and sensitive" probe of molecular interactions and dynamics. Both adjectives have at least two possible interpretations and, in fact, not all of them are strictly correct. First of all, the ^{17}O nucleus is certainly rare, as only 1 in 2600 oxygen atoms has the right number of neutrons to produce a magnetic response. This problem can sometimes be bypassed by working with isotopically enriched samples and, because of the improvements in the NMR instrumentation, also working with samples at natural ^{17}O abundance is not as problematic as is used to be. Secondly, ^{17}O NMR spectroscopy is also rare, in the sense that for a long time it has been practiced by a small, specialized community. However, it seems that this situation is changing rapidly, as demonstrated by the number of references in this review. This change has been stimulated by the need to improve our understanding of the structure, interactions and dynamics of oxygen-containing molecules, liquids (water), materials and biopolymers, or to design better MRI contrast agents. This review has shown that the newest, more advanced applications of liquid-state ^{17}O NMR have been made possible by the convergence of experimental methods, theoretical concepts and advanced computational tools. Thirdly, ^{17}O NMR is not really a sensitive technique, in the sense that the low receptivity of this nucleus implies low signal/noise ratios and long acquisition times. However, we hope to have convinced the reader that it is quite sensitive, in the sense that the positions and the widths of the NMR peaks arising from the ^{17}O nuclei are often very responsive to a change in the structure and molecular motions around them. Thus, recording and understanding an ^{17}O NMR spectrum is not always easy, but it can certainly be very informative and rewarding.

Author contributions. FC has mainly written Sections 2, 5, 6, AM has mainly written Section 4, GR has mainly written Sections 1, 3, 7 and overseen the whole work. All authors approve and share responsibility for the whole manuscript.

REFERENCES

[1] D. W. Boykin, ^{17}O NMR Spectroscopy in Organic Chemistry, CRC Press, 1991.

[2] I. P. Gerothanassis, Oxygen-17 NMR spectroscopy: Basic principles and applications (Part I), Progress in Nuclear Magnetic Resonance Spectroscopy 56 (2010) 95-197.

[3] I. P. Gerothanassis, Oxygen-17 NMR spectroscopy: Basic principles and applications (Part II), Progress in Nuclear Magnetic Resonance Spectroscopy 57 (2010) 1-110.

[4] X. H. Zhu, W. Chen, *In vivo* oxygen-17 NMR for imaging brain oxygen metabolism at high field, Progress in Nuclear Magnetic Resonance Spectroscopy 59 (2011) 319-335.

[5] E. Balogh, W. H. Casey, High-pressure ^{17}O NMR studies on some aqueous polyoxoions in water, Prog. Nucl. Magn. Reson. Spectrosc. 53 (2008) 193–207.

[6] K. Yamada, Recent Applications of Solid-State ^{17}O NMR, Annual Reports on NMR Spectroscopy 70 (2010) 215-258.

[7] V. Lemaître, M. E. Smith, A. Watts, A review of oxygen-17 solid-state NMR of organic materials - Towards biological applications, Solid State Nuclear Magnetic Resonance 26 (2004) 215-235.

[8] G. Wu, Solid-state ^{17}O NMR studies of organic and biological molecules, Progress in Nuclear Magnetic Resonance Spectroscopy 52 (2008) 118–169.

[9] A. Wong, F. Poli, Solid-State ^{17}O NMR Studies of Biomolecules, Annual Reports on NMR Spectroscopy 83 (2014) 145-220.

[10] S. E. Ashbrook, M. E. Smith, Solid state ^{17}O NMR - An introduction to the background principles and applications to inorganic materials, Chem. Soc. Rev. 35 (2006) 718-735.

[11] S. E. Ashbrook, S. Sneddon, New Methods and Applications in Solid-State NMR Spectroscopy of Quadrupolar Nuclei, J. Am. Chem. Soc. 136 (2014), 15440-15456.

[12] R.K. Harris, E.D. Becker, S.M. Cabral De Menezes, R. Goodfellow, P. Granger, NMR nomenclature. Nuclear spin properties and conventions for chemical shifts (IUPAC recommendations 2001), Pure Appl. Chem. 73 (2001) 1795–1818.

[13] A. Abragam, The Principles of Nuclear Magnetism, The International Series of Monographs on Physics, Oxford University Press, Oxford, 1961.

[14] C. P. Slichter, Principles of Magnetic Resonance, 3rd ed., Springer, Berlin, 1990.

[15] R. Ernst, G. Bodenhausen, and A. Wokaun, Principles of Nuclear Magnetic Resonance in One and Two Dimensions, The International Series of Monographs on Physics, Oxford University Press, Oxford, 1989.

[16] M. H. Levitt, Spin Dynamics, 2nd ed., J. Wiley and Sons, Chicester, 2008.

[17] A. Jerschow, From nuclear structure to the quadrupolar NMR interaction and high-resolution spectroscopy, Prog. Nucl. Magn. Res. Spectrosc. 46 (2005) 63-78.

[18] R. T. Boeré, R. G. Kidd, Rotational Correlation Times in Nuclear Magnetic Relaxation, Annual Reports on NMR Spectroscopy 13 (1983) 319-385.
[19] T. E. Bull, S. Forsen, D. L. Turner, TITLE, J. Chem. Phys. 70 (1979) 3106-3111.
[20] C. W. Chung and S. Wimperis, Measurement of spin-5/2 relaxation in biological and macromolecular systems using multiple-quantum NMR techniques, Mol. Phys. 76 (1992) 47-81.
[21] J. Zhu and G. Wu, Quadrupole central transition ^{17}O NMR spectroscopy of biological macromolecules in aqueous solution, J. Am. Chem. Soc. 133 (2011) 920–932.
[22] A. G. Refield, On the theory of relaxation processes, IBM J. Res. Devel. 1 (1957) 19-31.
[23] P. Westlund, H. Wennerström, NMR lineshapes of *I*=5/2 and *I*=7/2 nuclei. Chemical exchange effects and dynamic shifts, J. Magn. Reson. 50 (1982) 451-466.
[24] L. G. Werbelow, G. Pouzard, Quadrupolar relaxation. The multiquantum coherences, J. Phys. Chem. 85 (1981) 1357-1361.
[25] L. G. Werbelow, NMR Dynamic Frequency-Shift and the Quadrupolar Interaction, J. Chem. Phys. 70 (1979) 5381-5383.
[26] J. Zhu, E. Ye, V. Terskikh, G. Wu, Experimental Verification of the Theory of Nuclear Quadrupole Relaxation in Liquids over the Entire Range of Molecular Tumbling Motion, J. Phys. Chem. Lett. 2 (2011) 1020-1023.
[27] L. G. Werbelow, Adiabatic Nuclear Magnetic Resonance Line-width Contributions for Central Transitions of I>1/2 Nuclei, J. Chem. Phys. 104 (1996) 3457-3462.
[28] L. Lerner, D. A. Torchia, An analysis of non-Lorentzian sodium-23 line shapes in two model systems, J. Am. Chem. Soc. 108 (1986) 4264-4268.
[29] H. W. Spiess, NMR Principles and Progress, TITLE, Springer-Verlag Berlin, 15 (1978) 55-214.
[30] J. Kovalewski, L. Nordenskiold, N. Benetis, P. O. Westlund, Theory of nuclear spin relaxation in paramagnetic systems in solution, Prog. Nucl. Magn. Reson. Spectr. 17 (1985) 141-185.
[31] J.A. Peters, J. Huskens, D.J. Raber, Lanthanide induced shifts and relaxation rate enhancements, Prog. Nucl. Magn. Reson. Spectr. 28 (1996) 283-350.
[32] I. Bertini, C. Luchinat, NMR of paramagnetic substances, Coord. Chem. Rev. 150 (1996) 77-110.
[33] A. M. Achlama-Chmelnick, D. Fiat, Nuclear Magnetic Resonance Spectroscopy of Nuclei other than Protons, Wiley, London (1974) 143-152.
[34] R. Kimmich, Tomography, Diffusometry, Relaxometry, Springer, Berlin, 1997.
[35] I. Solomon, Relaxation processes in a system of two spins, Phys. Rev. 99 (1955) 559-565.

[36] N. Bloembergen, L. O. Morgan, Proton Relaxation Times in Paramagnetic Solutions. Effects of Electron Spin Relaxation, J. Chem. Phys. 34 (1961) 842-850.
[37] E. M. Gale, J. Zhu, and P. Caravan, Direct Measurement of the Mn(II) Hydration State in Metal Complexes and Metalloproteins through ^{17}O NMR Line Widths, J. Am. Chem. Soc. 135 (2013) 18600-18608.
[38] J. C. Miller, R. R. Sharp, Paramagnetic NMR relaxation enhancement: spin dynamics simulations of the effect of zero-field splitting interactions for S= 5/2, J. Phys. Chem. A 104 (2000) 4889-4895.
[39] J. Mares, M. Hanni, P. Lantto, J. Lounilaa and J. Vaara, Curie-type paramagnetic NMR relaxation in the aqueous solution of Ni(II), Phys. Chem. Chem. Phys. 16 (2014) 6916-6924.
[40] S. Aime, M. Botta, E. Terreno, P. L. Anelli and F. Uggeri, Gd(DOTP)$^{5-}$ outer-sphere relaxation enhancement promoted by nitrogen bases, Magn. Reson. Med. 30 (1993) 583-591.
[41] T. Helgaker, M. Jaszunski, K. Ruud, Ab initio methods for the calculation of NMR shielding and indirect spin-spin coupling constants, Chem. Rev. 99 (1999) 293-352.
[42] E. Oldfield, Quantum chemical studies of protein structure, Phil. Trans. R. Soc. B 360 (2005) 1347-1361.
[43] L. B. Casabianca, A. C. de Dios, Ab initio calculations of NMR chemical shifts, J. Chem. Phys. 128 (2008) 052201-1/10.
[44] C. Benzi, O. Crescenzi, M. Pavone, V. Barone, Reliable NMR chemical shifts for molecules in solution by methods rooted in density functional theory, Magn. Reson. Chem. 42 (2004) S57-S67.
[45] J. Vaara, Theory and computation of nuclear magnetic resonance parameters, Phys. Chem. Chem. Phys. 9 (2007) 5399-5418.
[46] J. C. Facelli, Chemical shift tensors: Theory and application to molecular structural problems, Prog. Nucl. Magn. Res. Spectr. 58 (2011) 176-201.
[47] M. W. Lodewyk, M. R. Siebert, D. J. Tantillo, Computational Prediction of ^{1}H and ^{13}C Chemical Shifts: A Useful Tool for Natural Product, Mechanistic, and Synthetic Organic Chemistry, Chem. Rev. 112 (2012) 1839-1862.
[48] C. Bonhomme, C. Gervais, F. Babonneau, C. Coelho, F. Pourpoint, T. Azaïs, S. E. Ashbrook, J. M. Griffin, J. R. Yates, F. Mauri, C. J. Pickard, First-Principles Calculation of NMR Parameters Using the Gauge Including Projector Augmented Wave Method: A Chemist's Point of View, Chem. Rev. 112 (2012) 5733-5779.
[49] M. Kaupp, M. Bühl, and V. G. Malkin, Calculations of NMR and EPR Parameters: Theory and Applications (Wiley-VCH, Weinheim, 2004).
[50] N. F. Ramsey, Magnetic shielding of nuclei in molecules, Phys. Rev. 78 (1955) 699-703.
[51] R. Ditchfield, Self-consistent perturbation theory of diamagnetism. I. A gauge-invariant LCAO method for NMR chemical shifts, Mol. Phys. 27 (1974) 789-807.

[52] K. Wolinski, J.F. Hinton, P. Pulay, Efficient implementation of the gauge independent atomic orbital method for NMR chemical shift calculations, J. Am. Chem. Soc. 112 (1990) 8251-8260.
[53] W. Kutzelnigg, U. Fleischer, M. Schindler, The IGLO-method: ab initio calculation and interpretation of NMR chemical shifts and magnetic susceptibilities, NMR Basic Princ. Prog. 23 (1990) 165-262.
[54] T. Helgaker, S. Coriani, P. Jørgensen, K. Kristensen, J. Olsen, K. Ruud, Recent advances in wave function-based methods of molecular-property calculations, Chem. Rev. 112 (2012) 543-631.
[55] W. Koch, M. C. Holthausen, A Chemist's Guide to Density Functional Theory, 2nd edition (Wiley-VCH, Weinheim, 2001).
[56] A. J. Cohen, P. Mori-Sanchez, W. Yang, Challenges for Density Functional Theory, Chem. Rev. 112 (2012) 289-320.
[57] S. Goedecker, Linear scaling electronic structure methods, Rev. Mod. Phys. 71 (1999), 1085-1123.
[58] S. Goedecker, G. Scuseira, Linear scaling electronic structure methods in chemistry and physics, Comput. Sci. Eng. 4 (2003), 14-21.
[59] C. Ochsenfeld, J. Kussmann and F. Koziol, Ab initio NMR spectra for molecular systems with a thousand and more atoms: a linear scaling method, Angew. Chem., Int. Ed. 43 (2004) 4485-4589.
[60] C. J. Cramer, D. G. Truhlar, Implicit solvation models: equilibria, structure, spectra, and dynamics, Chem. Rev. 99 (1999) 2161-2200.
[61] J. Tomasi, B. Mennucci, R. Cammi, Quantum mechanical continuum solvation models, Chem. Rev. 105 (2005) 2999-3093.
[62] M. J. Field, P. A. Bash, M. Karplus, A Combined Quantum-Mechanical and Molecular Mechanical Potential for Molecular-Dynamics Simulations. J. Comput. Chem. 11 (1990), 700-733.
[63] Q. Cui, M. Karplus, Molecular Properties from Combined QM/MM Methods. 2. Chemical Shifts in Large Molecules, J. Phys. Chem. B 104 (2000) 3721-3743.
[64] M. J. Field, A Practical Introduction to the Simulation of Molecular Systems, 2nd edition (Cambridge University Press, Cambridge, 2007).
[65] D. Marx, J. Hutter, Ab initio molecular dynamics: Theory and Implementation, in Modern Methods and Algorithms of Quantum Chemistry, J. Grotendorst (Ed.), NIC Series 1 (2000) 301-449.
[66] See www.gaussian.com (accessed on 23/11/2014).
[67] See www.msg.ameslab.gov/gamess/ (accessed on 23/11/2014).
[68] See www.nwchem-sw.org (accessed on 23/11/2014).
[69] See www.cec.mpg.de/forschung/molekulare-theorie-und-spektroskopie/orca.html (accessed on 23/11/2014).
[70] See www.turbomole.com (accessed on 23/11/2014).
[71] See www.schrodinger.com/Jaguar/ (accessed on 23/11/2014).

[72] See www.q-chem.com (accessed on 23/11/2014).
[73] See www.daltonprogram.org (accessed on 23/11/2014).
[74] See www.cfour.de (accessed on 23/11/2014).
[75] See http://www.scm.com/ADF/ (accessed on 23/11/2014).
[76] See www.cp2k.org (accessed on 23/11/2014).
[77] See www.quantumespresso.org (accessed on 23/11/2014).
[78] See www.castep.org (accessed on 23/11/2014).
[79] J. Gauss, Analytic second derivatives for the full coupled-cluster singles, doubles, and triples model: Nuclear magnetic shielding constants for BH, HF, CO, N_2, N_2O, and O_3, J. Chem. Phys. 116 (2002) 4773-4776.
[80] M. Kállay, J. Gauss, Analytic second derivatives for general coupled-cluster and configuration-interaction models, J. Chem. Phys. 120 (2004) 6841-6848.
[81] T. Kupka, Prediction of water's isotropic nuclear shieldings and indirect nuclear spin–spin coupling constants (SSCCs) using correlation-consistent and polarization-consistent basis sets in the Kohn–Sham basis set limit, Magn. Reson. Chem. 2009, 47, 210–221.
[82] E. Miliordos, S. S. Xantheas, On the Bonding Nature of Ozone (O_3) and Its Sulfur-Substituted Analogues SO_2, OS_2, and S_3: Correlation between Their Biradical Character and Molecular Properties, J. Am. Chem. Soc. 136 (2014) 2808-2817.
[83] R. E. Wasylishen, D. L. Bryce, A revised experimental absolute magnetic shielding scale for oxygen, J. Chem. Phys. 117 (2002) 10061-10066.
[84] K. Jackowski, M. Jaszunski, Nuclear Magnetic Moments from NMR Spectra ─ Experimental Gas Phase Studies and Nuclear Shielding Calculations, Concepts Magn. Res. 30A (2007) 246-260.
[85] A. A. Auer, High-level ab-initio calculation of gas-phase NMR chemical shifts and secondary isotope effects of methanol, Chem. Phys. Lett. 467 (2009) 230-232.
[86] W. Makulski, ^{1}H, ^{13}C, and ^{17}O nuclear magnetic shielding of methanol and its deuterated isotopomers from gas phase measurements, J. Mol. Struct. 872 (2008) 81-86.
[87] T. Kupka, Complete basis set prediction of methanol isotropic nuclear magnetic shieldings and indirect nuclear spin-spin coupling constants (SSCC) using polarization-consistent and XZP basis sets and B3LYP and BHandH density functionals, Magn. Reson. Chem., 47 (2009) 674-683.
[88] H. Sabzyan, B. Buzari, Theoretical study of the contribution of vibrational motions to nuclear shielding constants, Chem. Phys. 352 (2008) 297-305.
[89] J. Vaara, J. Lounila, K. Ruud, T. Helgaker, Rovibrational effects, temperature dependence, and isotope effects on the nuclear shielding tensors of water: A new ^{17}O absolute shielding scale, J. Chem. Phys. 109 (1998) 8388-8397.

[90] M. Makulski, M. Jaszunski, The ^{17}O nuclear magnetic shielding scale from gas-phase measurements, J. Mol. Struct. 651-653 (2003) 265-269.
[91] A. Bagno, F. Rastrelli, G. Saielli, NMR techniques for the investigation of solvation phenomena and non-covalent interactions, Prog. Nucl. Magn. Res. Spectrosc. 47 (2005) 41-93.
[92] A. D. Buckingham, Chemical Shifts in the Nuclear Magnetic Resonance Spectra of Molecules Containing Polar Groups, Can. J. Chem. 38 (1960) 300-307.
[93] J. Augspurger, J. G. Pearson, E. Oldfield, C. E. Dykstra, K. D. Park, D. Schwartz, Chemical-shift ranges in proteins, J. Magn. Res. 100 (1992) 342-357.
[94] H. C. Lee, E. Oldfield, Oxygen-17 Nuclear Magnetic Resonance Spectroscopic Studies of Carbonmonoxy Hemoproteins, J. Am. Chem. Soc. 111 (1989) 1584-1 590.
[95] E. Oldfield, H. C. Lee, C. Coretsopoulos, F. Adebodun, K. D. Park, S. Yang, J. Chung, B. Phillips, Solid-state Oxygen-17 Nuclear Magnetic Resonance Spectroscopic Studies of [$^{17}O_2$] Picket Fence Porphyrin, Myoglobin, and Hemoglobin, J. Am. Chem. Soc. 113 (1991) 8680-8685.
[96] M. Kaupp, C. Rovida, M. Parrinello, Density Functional Study of ^{17}O NMR Chemical Shift and Nuclear Quadrupole Coupling Tensors in Oxyheme Model Complexes, J. Phys. Chem. B 104 (2000) 5200-5208.
[97] P. Kukic, D. Farrell, L. P. McIntosh, B. García-Moreno E., K. Steen Jensen, Z. Toleikis, K. Teilum, J. E. Nielsen, Protein Dielectric Constants Determined from NMR Chemical Shift Perturbations, J. Am. Chem. Soc. 135 (2013) 16968-16976.
[98] A. Rizzo, J. Gauss, Shielding polarizabilities calculated at the coupled-cluster singles and doubles level augmented by a perturbative treatment of triple excitations, J. Chem. Phys. 119 (2002) 869-877.
[99] M. B. Ferraro, M. C. Caputo, G. I. Pagola, P. Lazzeretti, Electric quadrupole polarizabilities of nuclear magnetic shielding in some small molecules, J. Chem. Phys. 128 (2008) 044117-1/4.
[100] H. Kjær, S. P. A. Sauer, J. Kongsted, Benchmarking the multipole shielding polarizability/reaction field approach to solvation against QM/MM: Applications to the shielding constants of N-methylacetamide, J. Chem. Phys. 134 (2011) 044514-1/11.
[101] I. Alkorta, J. Elguero, P. F. Provasi, G. I. Pagola, M. B. Ferraro, Electric field effects on nuclear magnetic shielding of the 1:1 and 2:1 (homo and heterochiral) complexes of XOOX′ (X, X′ = H, CH3) with lithium cation and their chiral discrimination, J. Chem. Phys. 135 (2011) 104116-1/9.
[102] A. D. Buckingham, P. Fischer, Direct chiral discrimination in NMR spectroscopy, Chem. Phys. 324 (2006) 111-116.
[103] A. D. Buckingham, Permanent dipoles contribute to electric polarization in chiral NMR spectra, J. Chem. Phys. 140 (2014) 011103-1/3.
[104] T. M. Nymand, P.-O. Åstrand, Kurt V. Mikkelsen, Chemical Shifts in Liquid Water Calculated by Molecular Dynamics Simulations and Shielding Polarizabilities, J. Phys. Chem. B 101 (1997) 4105-4110.

[105] J. C. Hindman, Proton Resonance Shift of Water in the Gas and Liquid States, J. Chem. Phys. 44 (1966) 4582-4592.
[106] V. G. Malkin, O. L. Malkina, G. Steinebrunner, H Huber, Solvent effect on the NMR chemical shieldings in water calculated by a combination of molecular dynamics and density functional theory, Chem. Eur. J. 2 (1996) 452-457.
[107] B. G. Pfommer, F. Mauri, S. G. Louie, NMR Chemical Shifts of Ice and Liquid Water: The Effects of Condensation, J. Am. Chem. Soc. 122 (2000) 123-129.
[108] D. Sebastiani, M. Parrinello, Ab-initio Study of NMR Chemical Shifts of Water Under Normal and Supercritical Conditions, ChemPhysChem 3 (2002) 675-679.
[109] T. S. Pennanen, J. Vaara, P. Lantto, A. J. Sillanpää, Kari Laasonen, J. Jokisaari, Nuclear Magnetic Shielding and Quadrupole Coupling Tensors in Liquid Water: A Combined Molecular Dynamics Simulation and Quantum Chemical Study, J. Am. Chem. Soc. 126 (2004) 11093-11102.
[110] P. B. Karadakov, Electron correlation and basis set effects on the ^{17}O and ^{1}H nuclear magnetic shieldings in water clusters $(H_2O)_n$ (n=2-5), J. Mol. Struct. 602-603 (2002) 293-301.
[111] R. A. Klein, B. Mennucci, J. Tomasi, Ab Initio Calculations of ^{17}O NMR-Chemical Shifts for Water. The Limits of PCM Theory and the Role of Hydrogen-Bond Geometry and Cooperativity, J. Phys. Chem. A 108 (2004) 5851-5863.
[112] G. Bilalbegović, Nuclear Magnetic Resonance Parameters of Water Hexamers, J. Phys. Chem. A 114 (2010) 715-720.
[113] F. Castiglione, A. Baggioli, A. Citterio, A. Mele, G. Raos, Organic Peracids: A Structural Puzzle for ^{17}O NMR and Ab Initio Chemical Shift Calculations, J. Phys. Chem. A 116 (2012) 1814-1819.
[114] M. Cossi, O. Crescenzi, Different models for the calculation of solvent effects on ^{17}O nuclear magnetic shielding, J. Chem. Phys. 118 (2003) 8863-8872.
[115] M. Cossi, O. Crescenzi, Solvent effects on ^{17}O nuclear magnetic shielding: *N*-methylformamide in polar and apolar solutions, Theor. Chem. Acc. 111 (2004) 162-167.
[116] M. Pavone, O. Crescenzi, G. Morelli, N. Rega, V. Barone, Solvent effects on the UV ($n\rightarrow \pi^*$) and NMR (^{17}O) spectra of acetone in aqueous solution: development and validation of a modified Amber force field for an integrated MD/DFT/PCM approach, Theor. Chem. Acc. 116 (2006) 456-461.
[117] A. Baggioli, O. Crescenzi, M. J. Field, F. Castiglione, G. Raos, Computational ^{17}O-NMR spectroscopy of organic acids and peracids: comparison of solvation models, Phys. Chem. Chem. Phys. 15 (2013) 1130-1140.
[118] M. Dračínský, P. Bour, Computational Analysis of Solvent Effects in NMR Spectroscopy, J. Chem. Theory Comput. 6 (2010) 288-299.

[119] R. M. Gester, C. Bistafa, H. C. Georg, K. Coutinho, S. Canuto, Theoretically describing the ^{17}O magnetic shielding constant of biomolecular systems: uracil and 5-fluorouracil in water environment, Theor Chem Acc 133 (2014) 1424-
[120] J. J. P. Stewart, Optimization of parameters for semiempirical methods V: Modification of NDDO approximations and application to 70 elements, J. Mol. Model. 13 (2007) 1173-1213.
[121] R. F. W. Bader, Atoms in Molecules - A Quantum Theory, Oxford University Press, Oxford, 1990.
[122] M. D. Esrafili, A DFT investigation on hydrogen- and halogen-bonding interactions in dichloroacetic acid: application of NMR-GIAO and Bader theories, Struct. Chem. 24 (2013) 39-47.
[123] P. Siuda, J. Sadlej, Calculations of NMR properties for sI and sII clathrate hydrates of carbon dioxide, Chem. Phys. 433 (2014) 31-41.
[124] M. A. Collins, M. W. Cvitkovic, R. P. A. Bettens, The Combined Fragmentation and Systematic Molecular Fragmentation Methods, Acc. Chem. Res. 47 (2014) 2776-2785.
[125] H.-J. Tan, R. P. A. Bettens, Ab initio NMR chemical-shift calculations based on the combined fragmentation method, Phys. Chem. Chem. Phys. 15 (2013) 7541-7547.
[126] F. Mocci, Torsion angle relationship of the ^{17}O NMR chemical shift in α,β-unsaturated carbonyl compounds, Magn. Reson. Chem. 47 (2009) 862-867.
[127] F. Mocci, M. Usai, G. Cerioni, DFT and multinuclear magnetic resonance studies of diazenedicarboxylates and related compounds, Magn. Reson. Chem. 47 (2009) 31-37.
[128] F. Mocci, G. Uccheddu, A. Frongia, G. Cerioni, Solution Structure of Some λ^3 Iodanes: An ^{17}O NMR and DFT Study, J. Org. Chem. 74 (2009) 8818-8821.
[129] L. Fusaro, M. Luhmer, G. Cerioni, F. Mocci, On the Fluxional Behavior of Dess-Martin Periodinane: A DFT and ^{17}O NMR Study, J. Org. Chem. 72 (2007), 4163-4168.
[130] W. Makulski, A. Tulewicz, A. Leś, ^{17}O and ^{33}S nuclear magnetic shielding of sulfur trioxides from the experimental measurements and theoretical calculations, Magn. Reson. Chem. 52 (2014) 106-110.
[131] A. Pedone, M. Pavone, M. C. Menziani, V. Barone, Accurate First-Principle Prediction of ^{29}Si and ^{17}O NMR Parameters in SiO_2 Polymorphs: The Cases of Zeolites Sigma-2 and Ferrierite, J. Chem. Theory Comput. 4 (2008) 2130-2140.
[132] L. L. G. Justino, M. L. Ramos, F. Nogueira, A. J. F. N. Sobral, C. F. G. C. Geraldes, M. Kaupp, H. D. Burrows, C. Fiolhais, V. M. S. Gil, Oxoperoxo Vanadium(V) Complexes of L-Lactic Acid: Density Functional Theory Study of Structure and NMR Chemical Shifts, Inorg. Chem. 47 (2008) 7317-7326.
[133] A. Bagno, R. Bini, NMR Spectra of Terminal Oxo Gold and Platinum Complexes: Relativistic DFT Predictions, Angew. Chem. Int. Ed. 49 (2010) 1083-1086.
[134] M. Pascual-Borràs, X. López, A. Rodríguez-Fortea, R. J. Errington, J. M. Poblet, ^{17}O NMR chemical shifts in oxometalates: from the simplest monometallic species to mixed-metal polyoxometalates, Chem. Sci. 5 (2014) 2031-2042.

[135] J. Vaara, J. Jokisaari, R. E. Wasylishen, D. L. Bryce, Spin–spin coupling tensors as determined by experiment and computational chemistry, Prog. Nucl. Magn. Res. Spectrosc. 41 (2002) 233-304.
[136] T. Helgaker, M. Jaszunski, M. Pecul, The quantum-chemical calculation of NMR indirect spin–spin coupling constants, Prog. Nucl. Magn. Res. Spectrosc. 53 (2008) 249-268.
[137] B. Gierczyk, M. Kaźmierczak, Ł. Popenda, A. Sporzyński, G. Schroeder, S. Jurga, Influence of fluorine substituents on the NMR properties of phenylboronic acids, Magn. Reson. Chem. 52 (2014) 202-213.
[138] D. L. Bryce, A computational investigation of J couplings involving ^{27}Al, ^{17}O, and ^{31}P, Magn. Reson. Chem. 48 (2010) S69–S75.
[139] J. Autschbach, S. Zheng, R. W. Schurko, Analysis of Electric Field Gradient Tensors at Quadrupolar Nuclei in Common Structural Motifs, Concepts Magn. Res. 36A (2010) 84-126.
[140] A. Brown, R. E. Wasylishen, Nuclear Quadrupole Coupling Constants for N_2O: Experiment and Theory, J. Phys. Chem. A 116 (2012) 9769-9776.
[141] J. Schmidt, J. Hutter, H.-W. Spiess, D. Sebastiani, Beyond Isotropic Tumbling Models: Nuclear Spin Relaxation in Liquids from First Principles, ChemPhysChem 9 (2008) 2313-2316.
[142] M. D. Esrafili, Investigation of H-bonding and halogen-bonding effects in dichloroacetic acid: DFT calculations of NQR parameters and QTAIM analysis, J. Mol. Mod. 18 (2012) 2003–2011.
[143] D. J. Craik, R. T. C. Brownlee, Substituent effects on chemical shifts in the side chains of aromatic systems, Progr. Phys. Org. Chem. 14 (1983) 1-73.
[144] P. Balakrishnan, A.L. Baumstark, D. W. Boykin, Oxygen-17 NMR spectroscopy: effect of substituents on chemical shifts for para-substituted benzoic acids, methyl benzoates, cinnamic acids and methyl cinnamates, Org. Magn. Res. 22 (1984) 753-756.
[145] O. Exner, H. Dahn, P. Pechy, TITLE Magn. Res. Chem. 30 (1992) 381-386.
[146] M. Maccagno, A. Mele, R. Musio, G. Petrillo, F. Sancassan, O. Sciacovelli, D. Spinelli, TITLE Arkivoc 8 (2009) 212-221.
[147] V. Nummert, V. Mäemets, M. Piirsalu, I. A. Koppel, ^{17}O NMR studies of ortho-substituent effects in substituted phenyl tosylates, Magn. Reson. Chem. 50 (2012) 696-704.
[148] B. Gierczyk, M. Zalas, M. Kazmierczak, J. Grajewski, R. Pankiewicz, B. Wyrzykiewicz, TITLE Magn. Reson. Chem. 49 (2011) 648-654.
[149] R. Kiralj, M. M. C. Ferreira, Simple Quantitative Structure-Property Relationship (QSPR) Modeling of ^{17}O Carbonyl Chemical Shifts in Substituted Benzaldehydes Compared to DFT and Empirical Approaches, J. Phys. Chem. A 112 (2008) 6134-6149.

[150] G. Cerioni, E. Maccioni, M. C. Cardia, S. Vigo, F. Moccia, Characterization of 2,5-diaryl-1,3,4-oxadiazolines by multinuclear magnetic resonance and density functional theory calculations. Investigation on a case of very remote Hammett correlation, Magn. Reson. Chem. 47 (2009) 727-733.
[151] B. Gierczyk, M. Kazmierczak, G. Schroeder, A. Sporzynski, ^{17}O NMR studies of boronic acids and their derivatives, New J. Chem. 37 (2013) 1056-1072.
[152] A. Adamczyk-Woźniak, M. K. Cyranski, A. Dbrowśka, B. Gierczyk, P. Klimentowska, G. Schroeder, A. Zubrowska, A. Sporzynski, Hydrogen bonds in phenylboronic acids with polyoxaalkyl substituents at ortho-position, J. Mol. Struct. 920 (2009) 430-435.
[153] A. Adamczyk-Woźniak, K. M. Borys, K. Czerwińska, B. Gierczyk, M. Jakubczyk, I. D. Madura, A. Sporzynski, E. Tomecka, Intramolecular interactions in ortho-methoxyalkylphenylboronic acids and their catechol esters, Spectrochimica Acta 116 (2013) 616-621.
[154] J. Cerkovnik, B. Plesničar, Recent Advances in the Chemistry of Hydrogen Trioxide (HOOOH), Chem. Rev. 113 (2013) 7930-7951.
[155] B. Plesničar, T. Tuttle, J. Cerkovnik, J. Koller, D. Cremer, Mechanism of Formation of Hydrogen Trioxide (HOOOH) in the Ozonation of 1,2-Diphenylhydrazine and 1,2-Dimethylhydrazine: An Experimental and Theoretical Investigation, J. Am. Chem. Soc. 125 (2003) 11553-11564.
[156] J. Cerkovnik, B. Plesničar, J. Koller, T. Tuttle, Hydrotrioxides rather than cyclic tetraoxides (tetraoxolanes) as the primary reaction intermediates in the low-temperature ozonation of aldehydes. The case of benzaldehyde, J. Org. Chem. 74 (2009) 96-101.
[157] K. M. Błażewska, McKenna reaction — which oxygen attacks bromotrimethylsilane?, J. Org. Chem. 79 (2014) 408-412.
[158] R. E. Walstedt, Y. Tokunaga, S. Kambe, NMR studies of actinide oxides — A review, C. R. Physique 15 (2014) 563–572.
[159] T. Watanabe, Y. Ikeda, A Study on Identification of Uranyl Complexes in Aqueous Solutions Containing Carbonate Ion and Hydrogen Peroxide, Energy Procedia 39 (2013) 81–95.
[160] P. L. Zanonato, P. Di Bernardo, Z. Szabó, I. Grenthe, Chemical equilibria in the uranyl(VI)–peroxide–carbonate system; identification of precursors for the formation of poly-peroxometallates, Dalton Trans., 41 (2012) 11635-11641.
[161] N. Miyamoto, T. Tsukahara, Y. Kachi, M. Harada, Y. Kayaki, T. Ikariya, Y. Ikeda, Studies on solubility of uranyl complexes in supercritical carbon dioxide and its controlling factors using UV-visible and ^{17}O- and ^{19}F-NMR spectroscopy, J. Nucl. Sci. Technol., 49 (2012) 37-46.
[162] Z. Szabo, I. Furo and I. Csoregh, Combinatorial Multinuclear NMR and X-ray Diffraction Studies of Uranium(VI)-Nucleotide Complexes, J. Am. Chem. Soc. 127 (2005) 15236-15247.

[163] J. E. C. Wren, G. Schreckenbach, Neptunium(VII) in high-ionic-strength alkaline solutions - $[NpO_2(OH)_4]^{1-}$ or $[NpO_4(OH)_2]^{3-}$?, Can. J. Chem. 87 (2009) 1436-1443.
[164] H. Weingärtner, Understanding Ionic Liquids at the Molecular Level: Facts, Problems, and Controversies, Angew. Chem. Int. Ed. 47 (2008) 654-670.
[165] T. A. Zawodzinski, Jr. and R. A. Osteryoung Aspects of the Chemistry of Water in Ambient-Temperature Chloroaluminate Ionic Liquids: ^{17}O NMR Studies, Inorg. Chem. 26 (1987) 2920-2922.
[166] A. K. Abdul-Sada, A. G. Avent, M. J. Parkington, T. A. Ryan, K. R. Seddon and T. Welton Removal of Oxide Contamination from Ambient-temperature Chloroaluminate(III) Ionic Liquids J. Chem. Soc. Dalton Trans (1993) 3283-3286.
[167] S. Xu, Y. Lu, H. Wang, H. D. Abruna, L. A. Archer, A rechargeable Na–CO_2/O_2 battery enabled by stable nanoparticle hybrid electrolytes, J. Mater. Chem. A 2 (2014) 17723-17729.
[168] Z. Lin, M. L. Shelby, D. Hayes, K. A. Fransted, L. X. Chen, M. J. Allen, Water-exchange rate of lanthanide ions in an ionic liquid, Dalton Trans. 43 (2014) 16156-16159.
[169] X. Bogle, R. Vazquez, S. Greenbaum, A. von Wald Cresce, K. Xu, Understanding Li^+-Solvent Interaction in Nonaqueous Carbonate Electrolytes with ^{17}O NMR, J. Phys. Chem. Letters 4 (2013) 1664-1668.
[170] J. Chen, J.-Z. Yi, L.-M. Zhang, Water in Dextran Hydrogels, J. Appl. Polym. Sci. 117 (2010) 1631-1637.
[171] K. D. Park, K. Guo, F. Adebodun, M. L. Chiu, S. G. Sligar, E. Oldfield, Distal and Proximal Ligand Interactions in Heme Proteins: Correlations between C-0 and Fe-C Vibrational Frequencies, Oxygen-17 and Carbon-13 Nuclear Magnetic Resonance Chemical Shifts, and Oxygen-17 Nuclear Quadrupole Coupling Constants in $C^{17}O$- and ^{13}CO-Labeled Species, Biochemistry 30 (1991) 2333–2347.
[172] J. Zhu, I. C. M. Kwan, G. Wu, Quadrupole-Central-Transition ^{17}O NMR Spectroscopy of Protein-Ligand Complexes in Solution, J. Am. Chem. Soc. 131 (2009) 14206-14207.
[173] S. Hanashima, N. Fujiwara, K. Matsumoto, N. Iwasaki, G. Zheng, H. Torigoe, K. Suzuki, N. Taniguchi, and Y. Yamaguchi, A solution ^{17}O-NMR approach for observing an oxidized cysteine residue in Cu,Zn-superoxide dismutase, Chem. Commun. 49 (2013) 1449–1451.
[174] M. Lu, B. Atthe, G. D. Mateescu, C. a Flask, and X. Yu, Assessing mitochondrial respiration in isolated hearts using ^{17}O MRS, NMR Biomed., 25, (2012) 883–889.
[175] B. Prasad, D. J. Mah, A. R. Lewis, and E. Plettner, Water oxidation by a cytochrome P450: mechanism and function of the reaction, PLoS One 8 (2013) e61897.
[176] J. Qvist, C. Mattea, E. P. Sunde, B. Halle, Rotational dynamics in supercooled water from nuclear spin relaxation and molecular simulations, J. Chem. Phys. 136 (2012) 204505-1/16.

[177] B. Halle, Protein hydration dynamics in solution: a critical survey, Phil. Trans. R. Soc. Lond. B 359 (2004) 1207–1224.
[178] C. Mattea, J. Qvist, B. Halle, Dynamics at the Protein-Water Interface from ^{17}O Spin Relaxation in Deeply Supercooled Solutions, Biophys. J. 95 (2008) 2951-2963.
[179] E. Persson, B. Halle, Nanosecond to Microsecond Protein Dynamics Probed by Magnetic Relaxation Dispersion of Buried Water Molecules, J. Am. Chem. Soc. 130 (2008) 1774-1787.
[180] S. Kaieda, B. Halle, Internal Water and Microsecond Dynamics in Myoglobin, J. Phys. Chem. B 117 (2013) 14676−14687.
[181] F. Persson, B. Halle, Transient Access to the Protein Interior: Simulation versus NMR, J. Am. Chem. Soc. 135 (2013) 8735-8748.
[182] Y. Yan, X. Ou, H. Zhang, and Y. Shao, Effects of nano-materials on ^{17}O NMR line-width of water clusters, J. Mol. Struct., 1051 (2013) 211–214.
[183] V. M. Runge, M. A. Foster, J. A. Clanton, M. M. Jones, C. M. Lukehart, J. M. Hutchison, J. R. Mallard, F. W. Smith, C. L. Partain and A. E. James, Jr., TITLE, Radiology 152 (1984) 123–126.
[184] H.-J. Weinmann, R. C. Brasch, W.-R. Press and G. E. Wesbey, TITLE, Am. J. Roentgenol. 142 (1984) 619–624.
[185] A. Roca-Sabio, C. S. Bonnet, M. Mato-Iglesias, D. Esteban-Gómez, É. Tóth, A. de Blas, T. Rodríguez-Blas, and C. Platas-Iglesias, Lanthanide complexes based on a diazapyridinophane platform containing picolinate pendants. Inorg. Chem., 51(2012) 10893–903.
[186] A. M. Nonat, C. Gateau, P. H. Fries, L. Helm, and M. Mazzanti, New Bisaqua Picolinate-Based Gadolinium Complexes as MRI Contrast Agents with Substantial High-Field Relaxivities, Eur. J. Inorg. Chem. 2012 (2012) 2049–2061.
[187] A. E. Merbach, L. Helm, E. Toth, The chemistry of contrast agents in medical magnetic resonance imaging, (2013) 2nd edn. Wiley, New York.
[188] P. Hermann, J. Kotek, V. Kubíčeka, I. Lukeš, Gadolinium(III) complexes as MRI contrast agents: ligand design and properties of the complexes, Dalton Trans. 23 (2008) 3027-3047.
[189] A. Datta, K. N. Raymond, Gd−Hydroxypyridinone (HOPO)-Based High-Relaxivity Magnetic Resonance Imaging (MRI) Contrast Agents, Acc. Chem. Res. 42 (2009) 938-947.
[190] D. Delli Castelli, M. C. Caligara, M. Botta, E. Terreno, S. Aime, Combined high resolution NMR and ^{1}H and ^{17}O relaxometric study sheds light on the solution structure and dynamics of the Lanthanide(III) complexes of HPDO3A, Inorg. Chem. 52 (2013) 7130–7138.
[191] M. P. Placidi, M. Botta, F. K. Kálmán, G. E. Hagberg, Z. Baranyai, A. Krenzer, A. K. Rogerson, I. Tõth, N. K. Logothetis, G. Angelovski, Aryl-phosphonate lanthanide complexes and their fluorinated derivatives: Investigation of their unusual relaxometric behavior and potential application as dual frequency ^{1}H/^{19}F MRI probes, Chem. Eur. J. 19 (2013) 11644–11660.

[192] G. Tircsó, F. K. Kálmán, R. Pál, I. Bányai, T. R. Varga, R. Király, I. Lázár, L. Québatte, A. E. Merbach, É. Tóth, E. Brücher, Lanthanide Complexes Formed with the Tri- and Tetraacetate Derivatives of Bis(aminomethyl)phosphinic Acid: Equilibrium, Kinetic and NMR Spectroscopic Studies, Eur. J. Inorg. Chem. (2012) 2062–2073.
[193] B. Drahos, J. Kotek, P. Hermann, I. Lukes, E. Tóth, Mn(2+) complexes with pyridine-containing 15-membered macrocycles: thermodynamic, kinetic, crystallographic, and $^{1}H/^{17}O$ relaxation studies, Inorg. Chem. 49 (2010) 3224–3238.
[194] A. de Sá, C. S. Bonnet, C. F. G. C. Geraldes, É. Tóth, P. M. T. Ferreira, J. P. André, Thermodynamic stability and relaxation studies of small, triaza-macrocyclic Mn(II) chelates, Dalton Trans. 42 (2013) 4522–4532.
[195] V. Patinec, G. A. Rolla, M. Botta, R. Tripier, D. Esteban-Gómez, C. Platas-Iglesias, Hyperfine coupling constants on inner-sphere water molecules of a triazacyclononane-based Mn(II) complex and related systems relevant as MRI contrast agents, Inorg. Chem., 52 (2013) 11173–11184.
[196] G. A. Rolla, C. Platas-Iglesias, M. Botta, L. Tei, and L. Helm, ^{1}H and ^{17}O NMR Relaxometric and Computational Study on Macrocyclic Mn(II) Complexes, Inorg. Chem., 52 (2013) 3268–3279.
[197] L. Fusaro, F. Mocci, R. N. Muller, M. Luhmer, Insight into the dynamics of lanthanide-DTPA complexes as revealed by oxygen-17 NMR, Inorg. Chem. 51 (2012) 8455–8461.
[198] F. Mayer, C. Platas-Iglesias, L. Helm, J. A. Peters, K. Djanashvili, ^{17}O NMR and Density Functional Theory Study of the Dynamics of the Carboxylate Groups in DOTA Complexes of Lanthanides in Aqueous Solution, Inorg. Chem. 51 (2012) 170–178.
[199] L. Helm, A. E. Merbach, Inorganic and Bioinorganic Solvent Exchange Mechanisms, Chem. Rev. 105 (2005) 1923-1959.
[200] L. Helm, Ligand exchange and complex formation kinetics studied by NMR exemplified on fac-$[(CO)_3M(H_2O)]^+$ (M=Mn, Tc, Re), Coord. Chem. Rev. 252 (2008) 2346–2361.
[201] J. Maigut, R. Meier, A. Zahl, R. van Eldik, Triggering water exchange mechanisms via chelate architecture. Shielding of transition metal centers by aminopolycarboxylate spectator ligands, J. Am. Chem. Soc. 130 (2008). 14556–14569.
[202] D. Lieb, A. Zahl, T. E. Shubina, I. Ivanović-Burmazović, Water exchange on manganese(III) porphyrins. Mechanistic insights relevant for oxygen evolving complex and superoxide dismutation catalysis, J. Am. Chem. Soc. 132 (2010) 7282–7284.
[203] L. Helm, G. M. Nicolle, A. E. Merbach, Water and proton exchange processes on metal ions, Adv. Inorg. Chem. 57 (2005) 327-379.